JAERI-M
86-089

EVALUATION OF FUSION POWER MULTIPLICATION FACTOR

June 1986

Setsuo NIIKURA*, Masayuki NAGAMI
and Toshio HIRAYAMA

日本原子力研究所
Japan Atomic Energy Research Institute

JAERI-M レポートは，日本原子力研究所が不定期に公刊している研究報告書です。

入手の問合わせは，日本原子力研究所技術情報部情報資料課（〒319-11茨城県那珂郡東海村）あて，お申しこしください。なお，このほかに財団法人原子力弘済会資料センター（〒319-11 茨城県那珂郡東海村日本原子力研究所内）で複写による実費頒布をおこなっております。

JAERI-M reports are issued irregularly.

Inquiries about availability of the reports should be addressed to Information Division Department of Technical Information, Japan Atomic Energy Research Institute, Tokai-mura, Naka-gun, Ibaraki-ken 319-11, Japan.

編集兼発行　日本原子力研究所
印　　刷　㈱高野高速印刷

EVALUATION OF FUSION POWER MULTIPLICATION FACTOR

Setsuo NIIKURA*, Masayuki NAGAMI and Toshio HIRAYAMA

Department of Large Tokamak Research
Naka Fusion Research Establishment
Japan Atomic Energy Research Institute
Naka-machi, Naka-gun, Ibaraki-ken

(Received May 21, 1986)

The fusion power multiplication factor including the beam-plasma reaction (TCT effect), Q, has been evaluated with a simple plasma model, in which the radial profiles of the plasma temperature and density are taken to be typical forms observed in the recent experiments. The parameters to be varied in this model are $\bar{n}_e$, τ_E, beam power and energy, rf power, and impurity contents which affect the reduction of fueling density. For the typical application, we have investigated the operation window to attain a larger Q value for JT-60 hydrogen plasma which is converted to the equivalent deuterium-tritium plasma. When the TCT effect by 100 keV deuterium beam are considered, the minimum $n\tau T=2.7\times10^{23}$ ($\mathrm{sec\cdot eV\cdot m^{-3}}$) is necessary to achieve the break-even condition of JT-60. The Troyon β-limit is a crucial parameter in the break-even condition for a Ip=2 MA discharge if $\tau_E<0.55$ sec for 100 keV beam. The minimum $n\tau T$ required to attain the break-even condition is lowered by enhancement of the the beam-plasma reaction, by forming the peaked density and temperature profile, and by reducing the impurity contents. When the TCT effect by 200 keV deuterium beam are considered, the minimum $n\tau T$ can be lowered to 2.0×10^{23} ($\mathrm{sec\cdot eV\cdot m^{-3}}$).

Keywords: Fusion Power Multiplication Factor, Break-Even Condition, β-Limit, Beam-Plasma Reaction (TCT effect), $n\tau T$ Diagram

---

* On leave from Mitsubishi Atomic Power Industries, Inc.

核融合出力増倍率の評価

日本原子力研究所那珂研究所臨界プラズマ研究部
新倉節夫*・永見正幸・平山俊雄

（1986年5月21日受理）

核融合出力増倍率Q（TCT効果を含む）を，最近のトカマク実験の結果から得られたプラズマ温度・プラズマ密度の空間分布形を用いて，評価した。入力データは，τ_E，$\overline{n}_e$ NBIパワー，ビームエネルギ，RFパワーおよび不純物量である。代表的な計算例として，JT－60へ適用し，Qが大きい値をとる運転領域を探った。JT－60の水素プラズマは，等価なD－Tプラズマに換算して計算した。JT－60の臨界条件達成に必要な最小のn τ Tは，100 keVのNBIによるTCT効果を考慮すると，2.7×10^{23} (sec・eV・m^{-3}) である。ここで，I_p＝2MA放電では，τ_E＜0.55 secならば，Troyon β limitが，臨界条件達成の重要な因子となる。一方，ビーム・プラズマ反応の促進，プラズマ温度・プラズマ密度のピークした分布の形成，不純物量の低減などにより，臨界条件達成に必要なn τ Tは小さくなる。200keVのNBIによるTCT効果を考慮すると，最小のn τ Tは，2.0×10^{23} (sec・eV・m^{-3}) となる。

那珂研究所：〒311－02　茨城県那珂郡那珂町大字向山801番地の1
＊外来研究員：三菱原子力工業株式会社

Contents

目　　　次

1. INTRODUCTION

One of major objectives in recent large tokamaks like JT-60, TFTR and JET is to reach the plasma break-even condition. Simulations of the break-even condition utilizing the one-dimensional plasma transport code[1] or the high energy beam particle behavior code[2] generally take much CPU time. In these simulations, the energy confinement time and the plasma temperature or density profile cannot to be set individually since they are regulated by the electron thermal conductivities or the particle diffusion coefficient. Furthermore, some plasma parameters have uncertainties (for example the electron anomalous thermal conductivity, impurity accumulation and so on). In the present calculation, we employ a steady-state point model in which radial profiles of the plasma temperature and the electron density are assumed. These assumptions do not contradict with the profile consistency hypothesis.[3]

In the present paper, we find the operation window to achieve the plasma break-even condition considering two key factors, i.e., the energy confinement time and the β-limit. The results of the recent plasma experiments have made it clear that the β-limit depends on the plasma current linearly[4] and that its tendency follows the Troyon limit[5]. If the plasma current is suppressed to a lower value due to the machine limited conditions, the β-limit may not be expected to satisfy the break-even condition.

In Section 2, the calculational assumptions and equations are described. In Section 3, the typical calculational results of application to JT-60 are presented. In Section 4, the $n\tau T$ diagram calculated by the present model is discussed. In Section 5, the concluding remarks are summarized.

2. CALCULATIONAL METHOD

2.1 General Assumptions

The code described in this paper has been developed to calculate the fusion power multiplication factor, Q, taking into account the beam-plasma reaction (that is TCT effect).[6),7)] We assume electron temperature to be equal to ion temperature. The energy confinement time of thermal plasma, line averaged density, plasma current and auxiliary heating power are parameters for the Q investigation. Ohmic heating, beam heating, RF heating and α particle heating are considered as the plasma heating mechanism. Stored fast ion pressure and density produced by neutral beam injection and by α particle production are calculated based on the steady-state solution of the Fokker-Planck equation[(8)]. These assumptions seem to be valid under the condition that a beam heating pulse is longer than the fast ion slowing-down time and that the injected beam energy is larger than the thermal plasma kinetic energy. Fast ion production by RF heating is neglected in this code since these phenomena are not fully understood as yet. Only D-T fusion reaction is considered for the fusion power estimation. The hydrogen plasma is converted to the equivalent deuterium-tritium plasma, assuming that the proton density consists of the deuterium and tritium densities. The power multiplication factor for the beam-plasma reaction (TCT effect) is calculated assuming the Maxwellian target plasma and the beam velocity distribution.

The unit system in this calculation is MKS and eV.

The main flow chart of this code is presented in Appendix A.

2.2 General Equations

Following the assumptions in the previous section, general equations are described in this section.

Global energy balance is represented by

$$\frac{3}{2}\int\{n_e(r) + n_D^{th}(r) + n_T^{th}(r)\}\ T(r)\ dV$$

$$= \tau_E\ (P_{OH} + P_B^{abs} + P_{RF}^{abs} + P_\alpha) \tag{1}$$

where $n_e(r)$ is the electron density, $n_D^{th}(r)$ is the thermalized deuterium density, $n_T^{th}(r)$ is the thermalized tritium density, τ_E is the energy confinement time for the thermal plasma, P_{OH} is the ohmic heating power, P_B^{abs} is the absorbed neutral beam power, P_{RF}^{abs} is the absorbed RF power, P_α is the α particle heating power, and $T(r)=T_e(r)=T_i(r)$ is plasma temperature and its radial profile is assumed as follows;

$$T(r) = T^c\{(1 - (\frac{r}{a_p})^2)^{\frac{q_a}{\gamma} - 1}\}^{\frac{2}{3}} \tag{2}$$

where T^c is the plasma temperature at the plasma center, a_p is the plasma minor radius, $\gamma=q_o$ is the safety factor at the plasma center, and q_a is the safety factor at the plasma surface and given as follows;

$$q_a = \frac{2\pi\ B_t\ a_p^2}{\mu_0\ R_p\ I_p}\ \frac{1 + \kappa^2}{2} \tag{3}$$

where B_t is the toroidal magnetic field, R_p is the plasma major radius, I_p is the plasma current, and κ is the plasma ellipticity.

The radial profile of the electron density is assumed as follows;

$$n_e(r) = n_e^c \{ 1 - (\frac{r}{a_p})^4 \} \tag{4}$$

where n_e^c is the electron density at the plasma center. The thermalized deuterium and tritium densities are determined by the following equation;

$$n_e(r) = n_D^{th}(r) + n_T^{th}(r) + \bar{n}_B^f(r) + 2\bar{n}_\alpha^f(r) + Z_\ell n_{z\ell} + Z_m n_{zm} \tag{5}$$

where $\bar{n}_B^f(r)$ is the velocity space averaged fast ion density produced by neutral beam particles, $\bar{n}_\alpha^f(r)$ is the velocity space averaged fast ion density produced by α particles, Z_ℓ, $n_{z\ell}$ are the electric charge and density of a light impurity respectively, and Z_m, n_{zm} are for a metal impurity. The space profile of $n_{z\ell}/n_e$ and n_{zm}/n_e is assumed to be uniform. The velocity distribution of fast ions is assumed as follows;

$$f(v) \propto (v^3 + v_c^3)^{-1} \tag{6}$$

The velocity space averaged fast ion densities of the beam and α particles[8)] are described as follows;

$$\bar{n}^f(r) = \dot{S}(r) \cdot \tau_{se}(r) \int_0^{v_0} \frac{v^2}{v^3 + v_c(r)^3} dv \tag{7}$$

where $v_o = \sqrt{2E_B/m^f}$ is the initial velocity before the slowing-down process, E_B is the beam injection energy from the first to the third components, $\dot{S}(r)$ is the fast ion deposition rate (so called the birth rate) and profiles are presented in eq.(9)and eq.(10), and $\tau_{se}(r)$ is the Spitzer ion-electron momentum exchange time and given by

$$\tau_{se}(r) = 3.79 \times 10^{13} \frac{A_f \cdot T_e(r)^{\frac{3}{2}}}{Z_f^2 \cdot n_e(r)} \qquad (8)$$

where A_f is the atomic weight of the fast ion and Z_f is the electric charge of the fast ion. The radial profile of the beam deposition rate is assumed as follows;

$$\dot{S}_B(r) = \dot{S}_B^c \{1 - (\frac{r}{a})^2\}^\alpha \qquad (9)$$

where $\dot{S}_B^c$ is the beam birth rate at the plasma center. The profile of the α particle deposition rate is determined by the following equation;

$$\dot{S}_\alpha(r) = n_D^{th}(r) \cdot n_T^{th}(r) \cdot \langle\sigma v\rangle^{th}(r) + R_{B-P}(r) \qquad (10)$$

where $\langle\sigma v\rangle^{th}(r)$ is the fusion reactivity of the D-T thermal plasma and $R_{B-P}(r)$ is the beam-plasma reaction rate as described by eq.(19).

$V_c(r) = \sqrt{2E_c(r)/m^f}$ in eq.(7) is the critical velocity and E_c is the critical energy during the slowing-down process described as follows;

$$E_c(r) = 14.8T_e(r) \left(\frac{m_f}{m_H} \right)^{\frac{1}{3}} \left(\frac{m_f}{m_i} \right)^{\frac{2}{3}} \left(\frac{\sum_j n_j(r) \cdot Z_j^2 \cdot m_i}{\sum_j n_j(r) \cdot Z_j \cdot m_j} \right)^{\frac{2}{3}} \quad (11)$$

where the suffix f, H, j, i mean the fast ion, the hydrogen ion, the plasma ions and the typical ion, respectively, and m, n, and Z are mass, density and electric charge for each particle, respectively.

The α particle heating power without considering the orbit effect in eq.(1) is represented by

$$P_\alpha = 3.52(\mathrm{MeV}) \int \dot{S}_\alpha(r) dV \quad (12)$$

The volume averaged toroidal and poloidal beta value are presented as follows;

$$\langle\beta\rangle^{total} = \frac{\langle p\rangle^{th} + \langle p\rangle_B^f}{B_t^2/2\mu_0} \quad (13)$$

$$\beta_p^{total} = \frac{\langle p\rangle^{th} + \langle p\rangle_B^f}{B_p^2/2\mu_0} \quad (14)$$

where $\langle p\rangle^{th}$ is the volume averaged pressure of the thermal plasma, $\langle p\rangle_B^f$ is the volume averaged pressure of the beam fast ion derived from the assumption of one dimensional velocity distribution[8], and they are described by the following equation;

$$\langle p\rangle^{th} = \frac{\int \{n_e(r) + n_D^{th}(r) + n_T^{th}(r)\} T(r)\, dV}{V} \quad (15)$$

$$\langle p\rangle_B^f = \frac{\frac{2}{3}\int\{\dot{S}_B(r)\cdot\tau_{se}^B(r)\cdot E_B\cdot Ge(r)/2\}dV}{V} \tag{16}$$

where V is the total plasma volume and Ge is the energy transfered rate to plasma electrons during the slowing-down process given by

$$Ge(r) = \frac{2}{v_o^2}\int_0^{v_o}\frac{v^4}{v^3+v_c(r)^3}\,dv \tag{17}$$

The volume averaged pressure of the α particle fast ion which is derived by the similar equation to eq.(16) is neglected mainly in this calculation because of the smaller value compared with $\langle p\rangle_B^f$.

The fusion power multiplication factor including the beam-plasma reaction is described as follows;

$$Q^{total} = \frac{\int\{17.6(\mathrm{MeV})n_D^{th}(r)\cdot n_T^{th}(r)\cdot\langle\sigma v\rangle^{th}(r)+17.6(\mathrm{MeV})\cdot R_{B-P}(r)\}dV}{P_{OH}+P_B^{abs}+P_{RF}^{abs}} \tag{18}$$

The first term of the above equation is for the D-T thermal plasma reaction and the second is for the beam-plasma reaction. The beam-plasma reaction rate $R_{B-P}(r)$ is given by

$$R_{B-P}(r) = \dot{S}_B(r)\cdot n_t(r)\int_{E_{th}}^{E_B}\frac{\langle\sigma v\rangle_B}{-\langle\frac{dE}{dt}\rangle}\,dE \tag{19}$$

where $\langle\sigma v\rangle_B$ is the fusion reactivity between the Maxwellian thermal plasma and the mono-energy fast beam ion(see Appendx B).[7] $\langle\frac{dE}{dt}\rangle$ is the energy loss rate by all the thermal electron and ions (see

Appendix B) and derived from the assumption that the beam injection energy (E_B) is much larger than the thermal plasma energy (E_{th}).

3. APPLICATION TO JT-60

3.1 Plasma Parameter

The fusion power multiplication factor is studied for the JT-60 hydrogen plasma by converting it to the equivalent deuterium-tritium plasma. The typical plasma parameters of the JT-60 divertor plasma[9] used in the present calculation are described as follows;

R_p = 3.15 m

a_p = 0.83 m

V = 43 m^3

I_p = 2 MA (if possible 2.7 MA)

B_t = 4.3 T

q_0 = 0.9

P_B^{abs} = 20 MW

E_B = 100 keV

P_{RF}^{abs} = 10 MW

Z_ℓ = 8

$n_{z\ell}/n_e$ = 0.01

$Z_m = n_{zm}/n_e = 0$

The circular cross-section plasma is considered in this calculation. The auxiliary heating powers are treated as the absorbed power into plasma. The α particle heating is also considered as the plasma heating mechanism. The impurity contents in this case results in $Z_{eff} \sim 1.5$.

At first, we study the fusion power multiplication factor (Q) for the typical parameters of JT-60 in Sec. 3.2 ~ Sec. 3.4. Next, we investigate ways to enhance Q in Sec. 3.5 and Sec. 3.6 apprehending that the break-even condition could not be attained by the typical parameters. Finally, the effect of beam power deposition on Q is studied.

Fig. 1 indicates the radial profiles of various parameters in the typical calculational model. (τ_E=0.4s, $\bar{n}_e$=6×10¹⁹ m⁻³, E_B=100 keV, n_D^{th} : n_T^{th}=1:1, Q^{total}=0.94, and $\langle\beta\rangle^{total}$=2.34%).

3.2 Dependency on Plasma Density

The fusion multiplication factor including beam-plasma reaction (Q^{total}) versus the line averaged density ($\bar{n}_e$) is shown in Fig. 2 for the various auxiliary heating power at τ_E=0.4 sec and n_D^{th}:n_T^{th}=1:1. 20 MW of P_B^{abs} and additional 5 MW of P_{RF}^{abs} are required for Q^{total}> 1. In the case of P_B^{abs}= 20 MW, Q^{total} has the maximum value at $\bar{n}_e$=6×10⁻³ m⁻³. At this density, the fusion multiplication factor of the thermal plasma in eq.(18) is most enhanced since $\langle\sigma v\rangle^{th}$ has the square index dependency on the ion temperature between 10 keV and 20 keV under the same plasma pressure. The fusion multiplication factor by the beam-plasma reaction (Q^{beam}) is a half of Q^{total} at $\bar{n}_e$=6×10¹⁹ m⁻³. Q^{beam} for low density is larger than that for high density since R_{B-P} is enhanced by higher plasma temperature in low density (Fig.B-1).

Fig. 3 shows Q^{total} versus $\bar{n}_e$ with several values of τ_E at P_B^{abs} =20 MW and n_D^{th}:n_T^{th}=1:1. τ_E>0.4 sec is necessary for Q^{total}> 1. With τ_E=0.4 sec, Q^{total} has the maximum value at $\bar{n}_e$=6×10¹⁹ m⁻³ for the same reason as mentioned above.

3.3 Dependency on Energy Confinement Time

The dependence of Q^{total} on the energy confinement times is studied. Fig. 4 shows Q^{total}, $\langle\beta\rangle^{total}$, β_p^{total} and T^c versus τ_E at $\bar{n}_e=6\times10^{19}$ m^{-3}, $P_B^{abs}=20$ MW and $n_D^{th}:n_T^{th}=1:1$. These values increase monotonously with τ_E. The condition of Q^{total} beyond unit requires τ_E over 0.42 sec. The averaged toroidal beta, however, exceeds the Troyon beta limit at $\tau_E \geq 0.34$ sec for 2 MA of I_p and at $\tau_E \geq 0.45$ sec for 2.7 MA of I_p. The Troyon limit factor is assumed to be 3.5 based on the recent experiments[4]. We must note that Q and the averaged beta value for $I_p=2.7$MA are different more or less from them for $I_p=2$MA since the temperature profile is changed by q_a in eq.(2).

We study the dependencies of Q^{total} on Z_{eff} at $\bar{n}_e=6\times10^{19}$ m^{-3}, $P_B^{abs}=20$ MW and $n_D^{th}:n_T^{th}=1:1$, as shown in Fig. 5. We consider in this case $Z_\ell=6$ (carbon like) and $n_{z\ell}/n_e=0.01\sim0.06$ as the light impurity. The metal impurity is neglected. Q^{total} decreases with $n_{z\ell}/n_e$ since the thermal deuterium and tritium densities are reduced by the increase in impurity ions. In this case, $Z_{eff}<1.3$ is required for $Q^{total}>1$ at $\tau_E < 0.4$ s.

3.4 Q-$\langle\beta\rangle$ Diagram

According to the results described in the previous section, when the absorbed beam power is 20 MW and the energy confinement time is 0.4 sec, Q^{total} has the maximum value at 6×10^{19} m^{-3} of the line averaged electron density. So we have investigated the relation between Q^{total} and $\langle\beta\rangle^{total}$ for the various values of energy confiment time and auxiliary heating power at $\bar{n}_e=6.0\times10^{19}$ m^{-3} as shown in Fig. 6. Fig. 7 shows $Q^{thermal}$ which is obtained by subtracting the fusion multiplication factor by the beam-plasma reaction from Q^{total} in eq.(18) and $\langle\beta\rangle^{thermal}$ obtained by deducting the beam pressure from $\langle\beta\rangle^{total}$ in eq.(13).

The following are observed from Fig. 6 and Fig. 7. With $\tau_E \geq 0.80$ sec, $Q^{thermal} > 1$ is achievable for $P_B^{abs} < 10$ MW and $\langle\beta\rangle^{total} \sim 2\%$. With 0.55 sec $\leq \tau_E < 0.8$ sec, $Q^{total} > 1$ and $\langle\beta\rangle^{total} < 2\%$ is attained with $P_B^{abs} < 15$ MW, and $Q^{thermal} > 1$ is attainable for $P_B^{abs} = 20$ MW with added $P_{RF}^{abs} < 5$ MW while $\langle\beta\rangle^{total} > 2\%$. With 0.40 sec $< \tau_E < 0.55$ sec, $Q^{total} > 1$ is achievable for $P_B^{abs} = 20$ MW plus $P_{RF}^{abs} \sim 5$ MW while $\langle\beta\rangle^{total} > 2\%$. Consequently, if we consider the Troyon limit at I_p=2MA as the β-limit, $\tau_E \geq 0.55$ sec and $P_B^{abs} < 15$ MW are required for the break-even condition at $\bar{n}_e = 6\times10^{19}$ m^{-3}. With $\tau_E \leq 0.4$ sec, it is necessary to enhance Q value for the break-even condition in the way described in Sec. 3.5 and Sec. 3.6.

3.5 Enhancement of Beam-Plasma Reaction

The power multiplication factor of the beam-plasma reaction has a larger value with the beam energy, target plasma temperature and ratio of tritium to electron density increased as shown in Fig. B-1.

So we evaluate Q value for 200 keV deuterium beam with the same beam particle velocity as 100 keV hydrogen beam and for a low electron density ($\bar{n}_e = 4\times10^{19}$ m^{-3}) results in a higher target plasma temperature for the same plasma pressure. Fig. 8 shows Q^{total} as a function of the ratio of tritium density to the thermal dueterium and tritium densities for 100 keV and 200 keV deuterium beam, respectively. The minimum τ_E for $Q^{total} = 1$ in Fig. 8 is about 0.15 sec with $P_B^{abs} = 20$ MW and $n_T^{th}/(n_D^{th}+n_T^{th}) \sim 1$. The plasma radial profile for the minimum τ_E condition mentioned above is shown in Fig. 9. The thermal plasma pressure is comparable to the fast beam pressure. The density of the fast beam ion is a half the thermal tritium density.

3.6 Profile Effect

3.6.1 Plasma density

The effect of the electron density profile is studied for the following radial profile form.

$$n_e(r) = n_e^c \{1 - (\frac{r}{a})^2\}^\alpha \qquad (20)$$

Q^{total}, $Q^{thermal}$ and the plasma pressure versus the index α as a parameter at τ_E=0.4 sec, $\bar{n}_e=6\times10^{19}$ m^{-3}, P_B^{abs}= 20 MW and $n_D^{th}:n_T^{th}$=1:1 are shown in Fig. 10. With the peaked density profile as α increases, Q^{total} is large since the thermal plasma reaction is enhanced at the plasma center. On the other hand, the averaged plasma pressure is almost constant even if the electron density has the peaked profile. Consequently, when the density has the peaked profile by the beam or the pellet injected particles, Q is able to have a large value for the same τ_E and averaged toroidal beta. On this occasion, the central plasma temperature must keep the same high value even if the density profile changes.

3.6.2 Plasma Temperature

The effect of the plasma temperature profile is studied by the radial profile form of eq.(2). The radial density profile is given by eq.(4).

Q^{total}, $Q^{thermal}$ and the plasma pressure with the γ parameter of the plasma temperature at τ_E=0.4 sec, $\bar{n}_e$=6×10^{19} m^{-3}, P_B^{abs}=20 MW and n_D^{th}:n_T^{th}=1:1 are shown in Fig. 11. With γ=0.4 ~ 0.5, Q^{total} has the maximum value since the fusion reaction is enhanced at the plasma center. When the temperature profile is controlled by RF heating, Q is able to have a larger value with the same τ_E and $\langle\beta\rangle$.

3.7 Effect of Beam Deposition

The absorbed beam power has been assumed to be the injected beam power in the previous sections. The injected beam power is lost in the various forms such as shine through loss, charge exchange loss, orbit loss and ripple loss. In the case of the perpendicular injection to a low density plasma, the shine through loss is dominant. Fig. 12 shows the density dependence for the fusion multiplication factor, the averaged beta value and the absorbed power considering the beam shine through loss in the case of quasi-perpendicular injection, using the fast computer code for the beam deposition rate[10] at τ_E=0.4 sec, P_B^{inj}=20 MW, E_B=100 keV and n_D^{th}:n_T^{th} =1:1. Over twenty percents of the injection beam power is lost by the shine through at below 4×10^{19} m^{-3} of the line averaged electron density for 100 keV neutral beam. Then, the fusion multiplication factor and the averaged beta value decreases under 4×10^{19} m^{-3} of $\bar{n}_e$. Q has the maximum value at $\bar{n}_e$=6×10^{19} m^{-3} for the same reasons as mentioned in Sec. 3.2.

4. DISCUSSION

As the summary, we have calculated the $n\tau T$ diagram of the break-even condition and the ignition condition as shown in Fig. 13. The plasma temperature and density radial profiles are assumed to be eq.(2) and eq.(4), and Z_{eff}=1.5. In the present $n\tau T$ diagram, $\bar{n}_e$ is the line averaged electron density, τ_E is the energy confinement time of the thermal plasma, and $\bar{T}$ is the density averaged temperature. We consider three types of approaches to obtain the break-even condition. The first type is with the thermal D-T reaction only. The second and third ones are by the thermal reaction and the beam-plasma reaction utilized 100 keV and 200 keV dueterium beam, respectively. The values of the minimum $n\tau T$, which are required to satisfy the break-even condition, are 4.3×10^{23}, 2.7×10^{23}, 2.0×10^{23} ($\mathrm{sec\cdot eV\cdot m^{-3}}$) for each type as shown in Table 1. Each minimum $n\tau T$ is identified as A, B and C points in Fig. 13. If the profiles of the plasma temperature and density change from eq.(2) and eq.(4), described in Sec. 3.6, the minimum $n\tau T$ is different value. In the case of P_B^{abs}=20 MW and $n_D^{th}:n_T^{th}$ =1:1, $\bar{n}_e$, τ_E and $\bar{T}$ at the each minimum $n\tau T$ point are 7.4×10^{19} $\mathrm{m^{-3}}$, 0.54 sec and 10.7 keV for the first type, 6.3×10^{19} $\mathrm{m^{-3}}$, 0.42 sec and 10.4 keV for the second type, and 5.1×10^{19} $\mathrm{m^{-3}}$, 0.35 sec and 11.2 keV for the third type (Table 1). As far as the second type is concerned, the maximum Q at $\bar{n}_e$ ~ 6×10^{19} $\mathrm{m^{-3}}$, P_B^{abs}=20 MW, τ_E=0.4sec described in Sec. 3.2 exists close to the above minimum $n\tau T$. For reference, the minimum $n\tau T$ for ignition is 2.5×10^{24} ($\mathrm{sec\cdot eV\cdot m^{-3}}$).

We discuss the relation between the averaged toroidal beta value and the energy confinement time at the minimum $n\tau T$ values (Table 1) in

Fig. 14. $\langle\beta\rangle^{th'}$ in Fig. 14 means the plasma pressure where all particles are thermalized at B_T=4.3 T. The relation of τ_E and $\langle\beta\rangle^{th'}$ is described as follows;

$$\tau_E \propto \frac{[n\tau T]_{min}}{\langle\beta\rangle^{th'} \cdot B_t^2} \tag{21}$$

The absorbed power to the thermal plasma, P_{th}^{abs}, which is required for 43 m³ of the plasma volume is also indicated in Fig. 14, and represented by

$$P_{th}^{abs} \propto \frac{(\langle\beta\rangle^{th'})^2 \cdot B_t^4}{[n\tau T]_{min}} \tag{22}$$

The toroidal beta value is the important key parameter in the low plasma current if this value is restricted by the Troyon limit. We discuss the condition required to attain the break-even condition using the relation between $\langle\beta\rangle^{th'}$ and the Troyon β-limit. Since $\langle\beta\rangle^{th'}$ is used as a simple way instead of $\langle\beta\rangle^{total}$ which must be compared with the β-limit, the required conditions become loose more or less comparing with the condition described in Sec. 3.4. With Ip=2 MA, τ_E over 0.8 sec is required for only the D-T thermal plasma and the thermal absorbed power (P_{th}^{abs}) is required to be about 12 MW. On the other hand, if τ_E is below 0.8 sec, the beam-plasma reaction is needed. With the 100 keV deuterium beam, τ_E>0.5 sec and P_{th}^{abs} ~ 20 MW for I_p=2MA are required. With the 200 keV dueterium beam, τ_E > 0.35 sec and P_{th}^{abs}~26 MW for Ip=2 MA are required. In the case for $\tau_E \leq$ 0.35 sec, it is necessary to have the peaked density and temperature profile as represented in Sec. 3.6, to enhance the beam-plasma reaction described in Sec. 3.5 or to attain the larger beta value.[11]

The various τ_E scalings with the additional heating power and the plasma density are indicated in Fig. 15. Based on the results of the recent plasma experiments, the energy confinement time in the auxiliary heated plasma (so called L-mode)[12] is not so long compared with the expected value through the ohmic heated plasma[13]. Considering the previous studies, it is necessary to attain the high energy confinement time (so-called H-mode)[14] for achievement of the plasma break-even condition. If the energy confinement time increases with the plasma density like INTOR scaling, the minimum $n\tau T$ point shifts to the left-hand side along the each line. The minimum $n\tau T$ values with P_B^{abs}=20 MW for each type are 6.5×10^{23}, 4.3×10^{23}, 3.7×10^{23} ($sec\cdot eV\cdot m^{-3}$) in the τ_E-INTOR scaling.

5. CONCLUDING REMARKS

We have evaluated the fusion power multiplication factor with a simple plasma model as described the calculational assumptions and methods in Sec. 2. As the typical results, applications to the JT-60 plasma for the various parameter are presented. As the summary, we have shown the $n\tau T$ diagram obtained from the computed results. Consequently, it is concluded that the best approach to the break-even condition is to gain high energy confinement time (H-mode)[14)] or to increase β-limit[11)]. Alternative ways are to enhance the beam-plasma reaction, to form the peaked density and temperature profile, or to reduce impurity contents.

Acknowledgements

The authors are grateful to Dr. T. Tone for his help in calculating the beam-plasma reaction. The authors wish to express their gratitude to Drs. S. Seki, H. Ninomiya, R. Yoshino, K. Shimizu and M. Kikuchi for useful discussions. The authors would like to gratefully acknowledge the encouragement and support by Drs. M. Yoshikawa, S. Tamura, Y. Suzuki, Y. Shimomura, M. Azumi and the staff of the JT-60 team.

5. CONCLUDING REMARKS

We have evaluated the fusion power multiplication factor with a simple plasma model as described the calculational assumptions and methods in Sec. 2. As the typical results, applications to the JT-60 plasma for the various parameter are presented. As the summary, we have shown the $n\tau T$ diagram obtained from the computed results. Consequently, it is concluded that the best approach to the break-even condition is to gain high energy confinement time (H-mode)[14] or to increase β-limit[11]. Alternative ways are to enhance the beam-plasma reaction, to form the peaked density and temperature profile, or to reduce impurity contents.

Acknowledgements

The authors are grateful to Dr. T. Tone for his help in calculating the beam-plasma reaction. The authors wish to express their gratitude to Drs. S. Seki, H. Ninomiya, R. Yoshino, K. Shimizu and M. Kikuchi for useful discussions. The authors would like to gratefully acknowledge the encouragement and support by Drs. M. Yoshikawa, S. Tamura, Y. Suzuki, Y. Shimomura, M. Azumi and the staff of the JT-60 team.

References

1) Hirayama, T., et. al., JAERI-M 82-204 (1982).

2) Tani, K., et. al., Heating in Toroidal Plasma (Proc. Joint Varrena-Grenoble Int. symp. 1978), vol. 1 (1978) 31

3) Murakami, M., et. al., Controlled Fusion and Plasma Physics (Proc. 12th Europ. Conf. Budapest, 1985), Invited Paper (1985) 17.

4) Stambaugh, R.D., Moore, R.W., Bernard, L.C., Kellman, A.G., Strait, E.J., et. al., Plasma Physics and Controlled Nuclear Fusion Research (Proc. 10th Int. Conf. London, 1984) Vol. 1, IAEA, Vienna (1985) 217.

5) Troyon, F., Gruber, R., Saurenmann, H., Semenzato, S. and Succi, S., Plasma Phys. Contr. Fusion 26 (1984)209.

6) Dawson, J.M., Furth, H.P. and Tenney, F.H. Phys. Rev. Lett. 26 (1971) 1156.

7) Tone, T., JAERI-M 7769 (1978).

8) Callen, J.D., Colchin, R.J., Fowler, R.H., McAlees, D.G. and Rome, J.A., Plasma Physics and Controlled Nuclear Fusion Research (Proc. 5th Int. Conf. Tokyo, 1974) Vol. 1, IAEA, Vienna (1975) 645.

9) JT-60 Team, Controlled Fusion and Plasma Physics (Proc. 12th Europ. Conf. Budapest, 1985), Invited Paper (1985) 165.

10) Otsuka, M., Nagami, M. and Matsuda, T., JAERI-M 82-129 (1982).

11) Seki, S., and Azumi, M., JAERI-M 86-025 (1986).

12) Kaye, S.M., and Goldstron, R.J., Nucl. Fusion 25 (1985) 65.

13) Efthimion, P., Bell, M., Blanchard, W., Bretz, N., Cecchi, J., et al., Phys. Rev. Lett. 52 (1984) 1492.

14) Wagner, F., Becker, G., Behringer, K., Campbell, D., Eberhagen, A., et al., Phys. Rev. Lett. 49 (1982) 1408.

FIGURE CAPTIONS

FIG. 1 Typical radial profiles of plasma density (n_e, n_D^{th}, n_T^{th}), stored fast ion density ($\bar{n}_B^f$, $\bar{n}_\alpha^f$), plasma temperature (T), velocity space averaged beam and α particle energy ($\bar{E}_B^f$, $\bar{E}_\alpha^f$), thermal plasma pressure (p^{th}), and velocity space averaged beam fast ion pressure ($\bar{p}_B^f$) at τ_E=0.4 sec, $\bar{n}_e$=6×10^{19} m^{-3}, P_B^{abs}(=20 MW) + P_α, E_B=100 keV, n_D^{th}:n_T^{th}=1:1, R_p=3.15 m, a_p=0.83 m, B_T=4.3 T and I_p=2 MA resulting Q^{total}=0.94 and $\langle\beta\rangle^{total}$=2.34%.

FIG. 2 Dependency of Q^{total} on the plasma density as a function of various auxiliary heating power at τ_E=0.4sec, E_B=100 keV, n_D^{th}:n_T^{th}=1:1, R_p=3.15 m, a_p=0.83 m, B_T=4.3 T and I_p=2 MA. Line averaged electron densities for Murakami factors which correspond to 6.0 and 10.0 are also indicated.

FIG. 3 Dependency of Q^{total} on plasma density as a function of energy confinement time at P_B^{abs}(=20MW)+P_α, E_B=100 keV, n_D^{th}:n_T^{th}=1:1, R_p=3.15 m, a_p=0.83 m, B_T=4.3T and I_p=2 MA. Line averaged electron densities for Murakami factors which correspond to 6.0 and 10.0 are also indicated.

FIG. 4 Dependency of Q^{total}, $Q^{thermal}$, $\langle\beta\rangle^{total}$, β_p^{total} and T^c on energy confinement time at $\bar{n}_e$=6×10^{19} m^{-3}, P_B^{abs}(=20 MW) + P_α, E_B=100 keV, n_D^{th}:n_T^{th}=1:1, R_p=3.15 m, a_p=0.83 m, B_T=4.3T and q_a=2.34. Troyon β-limits for I_p=2 MA and 2.7 MA are also indicated.

FIG. 5 Dependency of Q^{total} on energy confinement time with various $n_{z\ell}/n_e$ at Z_ℓ=6, $\bar{n}_e$=6×10^{19} m^{-3}, P_B^{abs}(=20 MW) + P_α, E_B=100 keV,

$n_D^{th}:n_T^{th}$ =1:1, R_p=3.15 m, a_p=0.83 m, B_T=4.3 T and I_p=2 MA. Metal impurity is neglected.

FIG. 6 Q^{total} versus $\langle\beta\rangle^{total}$ at $\bar{n}_e=6\times10^{19}$ m^{-3}, E_B=100 keV, $n_D^{th}:n_T^{th}$ =1:1, R_p=3.15 m, a_p=0.83 m, B_T=4.3T and q_a=2.34. Solid lines indicate τ_E constant case. Dashed lines denote auxiliary heating power constant case. Troyon β-limits for I_p=2 MA and 2.7 MA are also indicated.

FIG. 7 $Q^{thermal}$ versus $\langle\beta\rangle^{thermal}$ at $\bar{n}_e=6\times10^{19}$ m^{-3}, E_B=100 keV, $n_D^{th}:n_T^{th}$=1:1, R_p=3.15 m, a_p=0.83 m, B_T=4.3T and q_a=2.34. Solid lines indicate τ_E constant case. Dashed lines denote auxiliary heating power constant case. Troyon β-limits for I_p=2 MA and 2.7 MA are also indicated.

FIG. 8 Q^{total} as a function of $n_T^{th}/(n_D^{th}+n_T^{th})$ which is the ratio of tritium density to deuterium plus tritium densities as a function of various energy confinement times at $\bar{n}_e=4\times10^{19}$ m^{-3}, P_B^{abs}(=20 MW) + P_α, R_p=3.15 m, a_p=0.83 m, B_T=4.3T and I_p=2 MA. Q^{total} by 100 keV deuterium beam is indicated by dashed line and that by 200 keV deuterium beam is represented by solid line.

FIG. 9 Radial profiles of plasma density (n_e, n_D^{th}, n_T^{th}), stored fast ion density ($\bar{n}_B^f$, $\bar{n}_\alpha^f$), plasma temperature (T), velocity space averaged beam and α particle energy ($\bar{E}_B^f$, $\bar{E}_\alpha^f$), thermal plasma pressure (p^{th}), and velocity space averaged beam fast ion pressure ($\bar{p}_B^f$) at τ_E=0.15 sec, $\bar{n}_e=4\times10^{19}$ m^{-3}, P_B^{abs}(=20MW)+P_α, E_B=200 keV, $n_D^{th}:n_T^{th}$=0:1, R_p=3.15 m, a_p=0.83 m, B_T=4.3T and I_p=2 MA resulting Q^{total}=0.98 and $\langle\beta\rangle^{total}$=1.54%.

FIG. 10 (a) Dependency of Q^{total}, $Q^{thermal}$, $\langle\beta\rangle^{total}$, β_p^{total} and T^c on density index α at τ_E=0.4 sec, $\bar{n}_e$=6×10¹⁹ m⁻³, P_B^{abs} (=20MW)+P_α, E_B=100 keV, $n_D^{th}:n_T^{th}$=1:1, R_p=3.15 m, a_p=0.83 m, B_T=4.3 T and I_p=2 MA. (b) Typical radial profiles of electron densities with index α.

FIG. 11 (a) Dependency of Q^{total}, $Q^{thermal}$, $\langle\beta\rangle^{total}$, β_p^{total} and T^c on plasma temperature radial profile parameter γ at τ_E=0.4 sec, $\bar{n}_e$=6×10¹⁹ m⁻³, P_B^{abs}(=20MW)+P_α, E_B=100 keV, $n_D^{th}:n_T^{th}$=1:1, R_p=3.15 m, a_p=0.83 m, B_T=4.3 T and I_p=2 MA. (b) Typical radial profiles of plasma temperature with parameter γ by solid lines. Dashed line shows radial profile of electron density.

FIG. 12 Effect of beam deposition. Density dependence of Q^{total}, $Q^{thermal}$, $\langle\beta\rangle^{total}$, β_p^{total}, T^c, absorbed power into plasma P^{abs} and shine through loss P_s at τ_E=0.4 sec, P_B^{inj}(=20MW)+P_α, E_B=100 keV, $n_D^{th}:n_T^{th}$=1:1, R_p=3.15 m, a_p=0.83 m, B_T=4.3 T and I_p=2 MA. We neglect charge exchange loss, orbit loss and ripple loss. Line averaged electron densities for Murakami factors which correspond to 6.0 and 10.0 are also indicated.

FIG. 13 $n\tau T$ diagram for ignition condition and break-even conditions. We consider three break-even conditions by only thermal D-T reaction and by thermal D-T reaction including TCT effect with 100 keV and 200 keV deuterium beam at Z_{eff}=1.5 and $n_T^{th}/(n_T^{th}+n_D^{th})$=0.5. Point where each condition's line touches $n\tau T$ constant line has the minimum $n\tau T$ value and is indicated as symbol A, B, C and I. Q^{total}=1 considering TCT effect with 200 keV deuterium beam for $n_T^{th}/(n_T^{th}+n_D^{th})$=0.75 or 1.0 is also indicated.

FIG. 14 Relation between energy confinement time and averaged toroidal beta values which means the plasma pressure where all particles are thermalized at B_T=4.3 T for the minimum $n\tau T$ values by only thermal D-T reaction and by thermal D-T reaction including TCT effect with 100 keV and 200 keV deuterium beam. Absorbed power to thermal plasma P_{th}^{abs} for 43 m^3 of plasma volume is also indicated.

FIG. 15 Various τ_E scaling. (a) Power dependence at $\bar{n}_e$=6×10^{19} m^{-3}, R_p=3.15 m, a_p=0.83 m, B_T=4.3 T and I_p=2 MA. (b) Density dependence at P^{abs}=20 MW, R_p=3.15 m, a_p=0.83 m, B_T=4.3 T and I_p=2 MA. Kaye-Goldston × 2 suggests H-mode scaling.

FIG.B-1 Power multiplication factor of the beam-plasma reaction Q_B as a function of deutron injection energy for various plasma temperatures (T_e=T_i) in a Maxwellian target plasma. The case of n_T^{th}=n_e is indicated by solid lines and the case of n_T^{th}=n_D^{th}=n_e/2 is demonstrated by dashed lines. 17.6 MeV per reaction.

Table 1 The minimum $n\tau T$ values and $\bar{n}_e$, τ_E, $\bar{T}$ required to attain the break-even condition in the case of P_B^{abs}(=20 MW)+P_α and $n_D^{th}:n_T^{th}=1:1$

	Type	the minimum $n\tau T$ (sec.eV.m^{-3})	$\bar{n}_e$ (m^{-3})	τ_E (sec)	$\bar{T}$ (keV)
A	only thermal plasma	4.3×10^{23}	7.4×10^{19}	0.54	10.7
B	thermal plasma + TCT (100 keV)	2.7×10^{23}	6.3×10^{19}	0.42	10.4
C	thermal plasma + TCT (200 keV)	2.0×10^{23}	5.1×10^{19}	0.35	11.2
I	ignition	2.5×10^{24}			

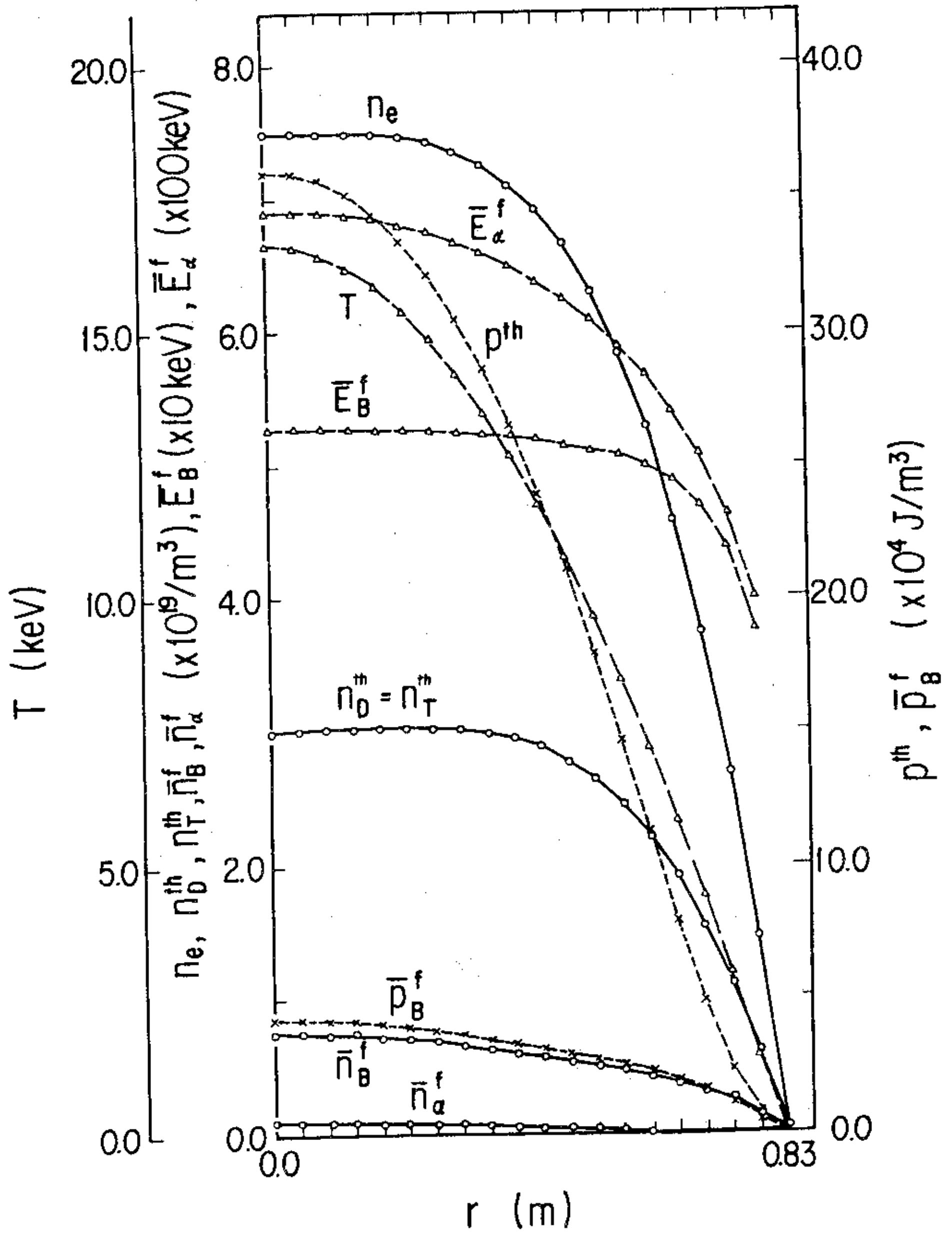

FIG. 1 Typical radial profiles of plasma density (n_e, n_D^{th}, n_T^{th}), stored fast ion density ($\bar{n}_B^f$, $\bar{n}_\alpha^f$), plasma temperature (T), velocity space averaged beam and α particle energy ($\bar{E}_B^f$, $\bar{E}_\alpha^f$), thermal plasma pressure (p^{th}), and velocity space averaged beam fast ion pressure ($\bar{p}_B^f$) at τ_E=0.4 sec, $\bar{n}_e$=6×10¹⁹ m⁻³, P_B^{abs}(=20 MW) + P_α, E_B=100 keV, n_D^{th}:n_T^{th}=1:1, R_p=3.15 m, a_p=0.83 m, B_T=4.3 T and I_p=2 MA resulting Q^{total}=0.94 and $\langle\beta\rangle^{total}$=2.34%.

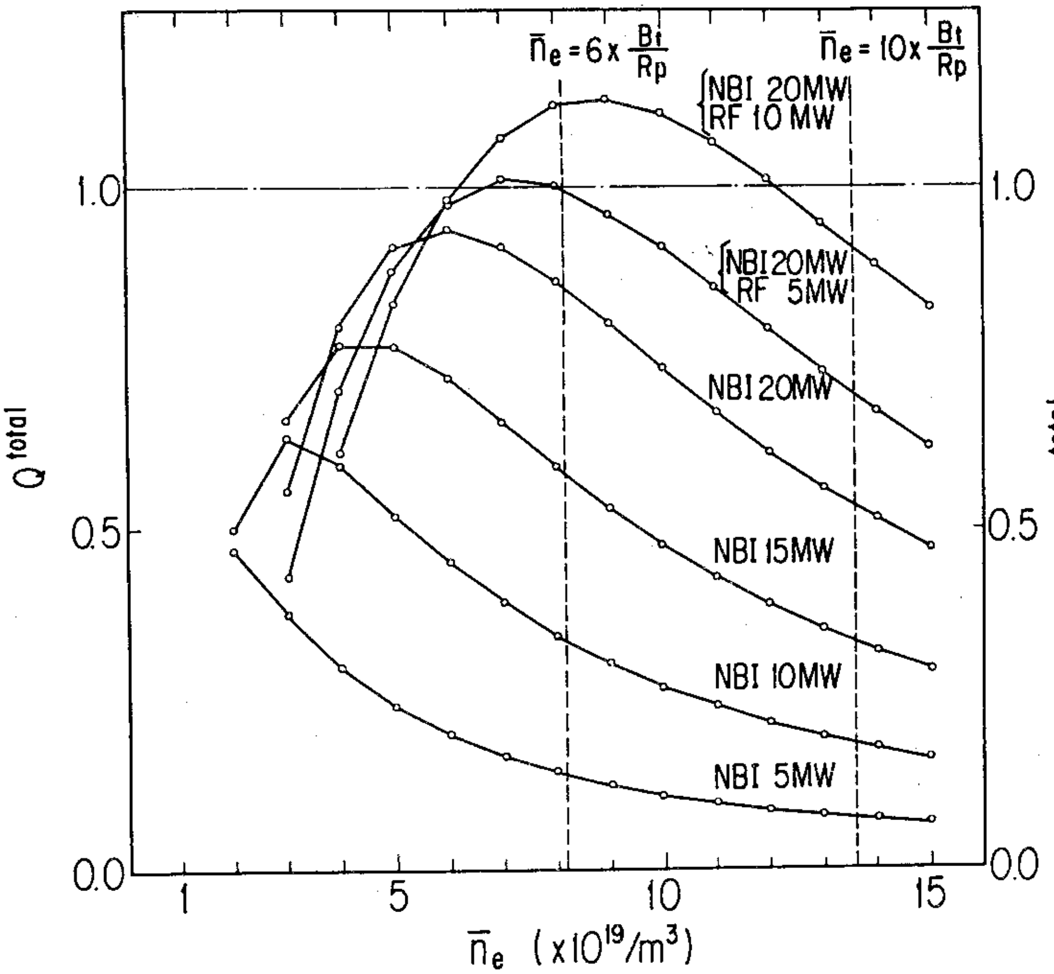

FIG. 2 Dependency of Q^{total} on the plasma density as a function of various auxiliary heating power at τ_E=0.4sec, E_B=100 keV, $n_D^{th}:n_T^{th}$=1:1, R_p=3.15 m, a_p=0.83 m, B_T=4.3 T and I_p=2 MA. Line averaged electron densities for Murakami factors which correspond to 6.0 and 10.0 are also indicated.

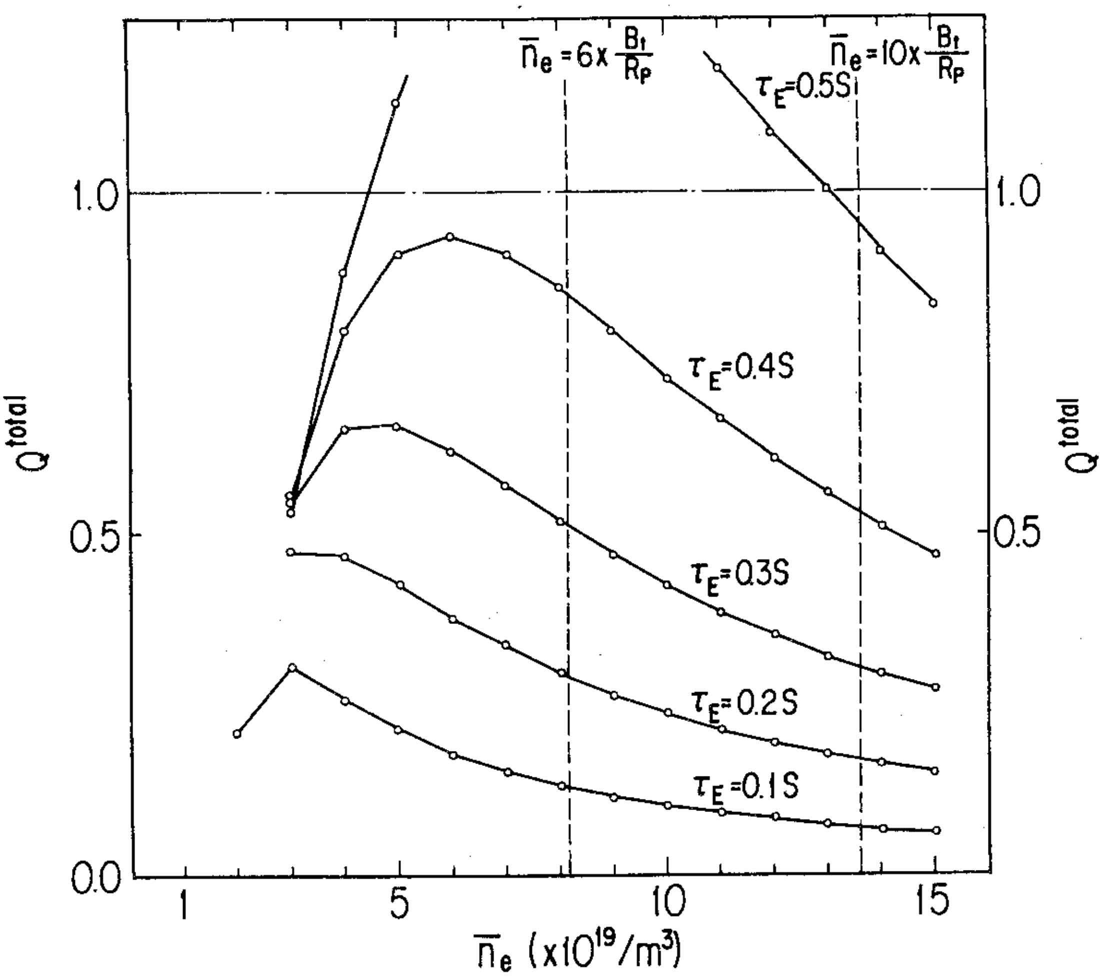

FIG. 3 Dependency of Q^{total} on plasma density as a function of energy confinement time at P_B^{abs}(=20MW)+P_α, E_B=100 keV, n_D^{th}:n_T^{th}=1:1, R_p=3.15 m, a_p=0.83 m, B_T=4.3T and I_p=2 MA. Line averaged electron densities for Murakami factors which correspond to 6.0 and 10.0 are also indicated.

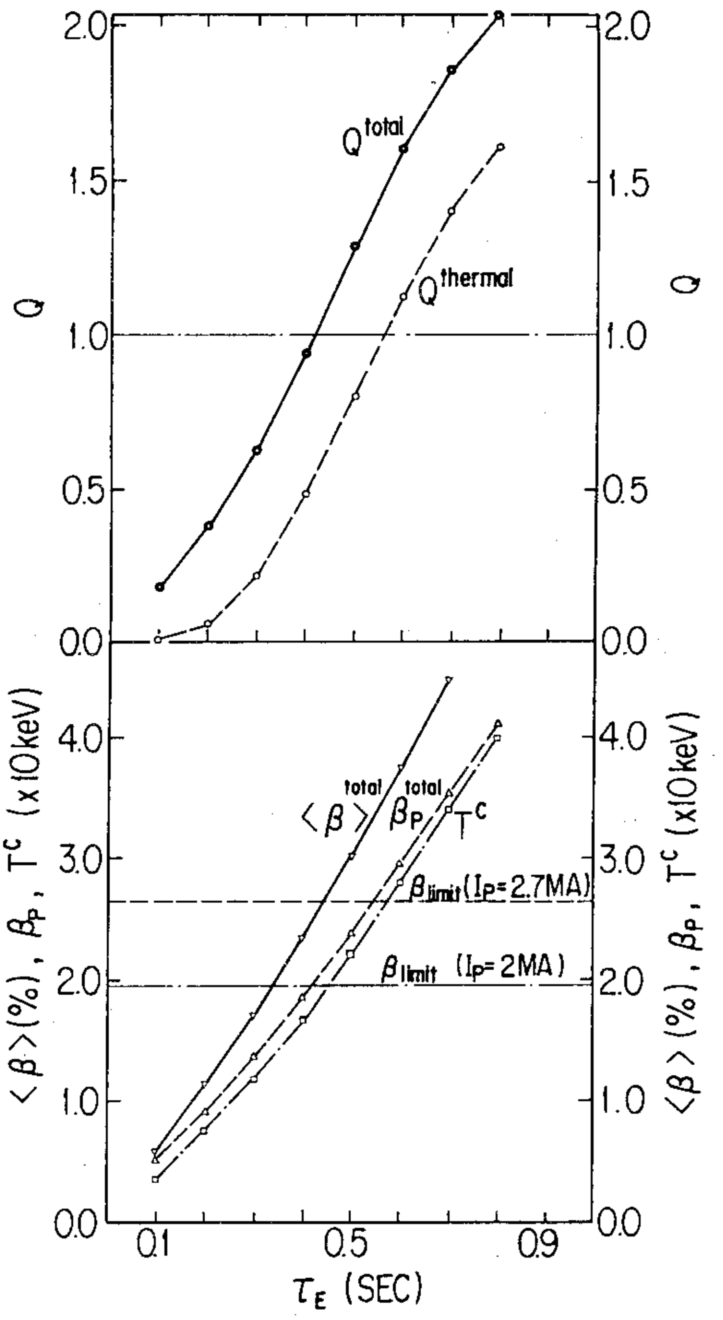

FIG. 4 Dependency of Q^{total}, $Q^{thermal}$, $\langle\beta\rangle^{total}$, β_p^{total} and T^c on energy confinement time at $\bar{n}_e$=6×10¹⁹ m⁻³, P_B^{abs}(=20 MW) + P_α, E_B=100 keV, n_D^{th}:n_T^{th}=1:1, R_p=3.15 m, a_p=0.83 m, B_T=4.3T and q_a=2.34. Troyon β-limits for I_p=2 MA and 2.7 MA are also indicated.

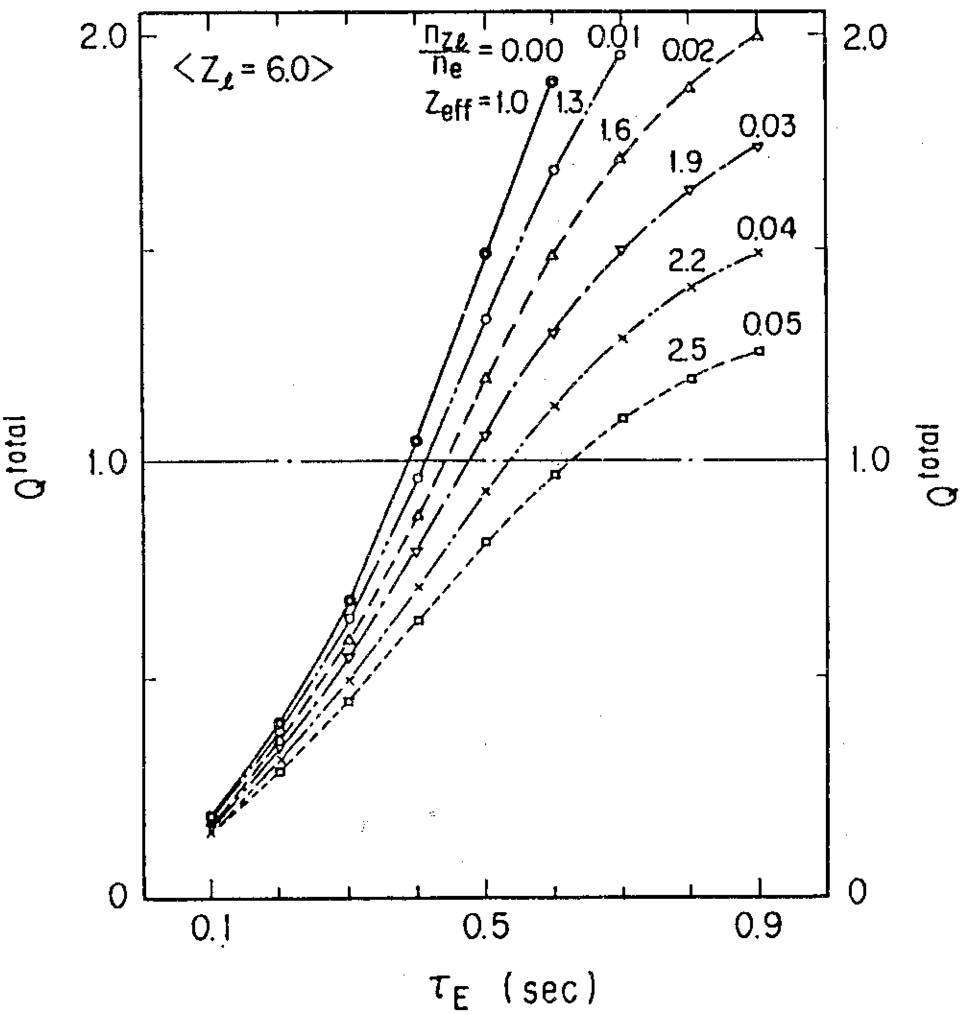

FIG. 5 Dependency of Q^{total} on energy confinement time with various $n_{z\ell}/n_e$ at $Z_\ell=6$, $\bar{n}_e=6\times10^{19}$ m^{-3}, P_B^{abs}(=20 MW) + P_α, E_B=100 keV, $n_D^{th}:n_T^{th}$ =1:1, R_p=3.15 m, a_p=0.83 m, B_T=4.3 T and I_p=2 MA. Metal impurity is neglected.

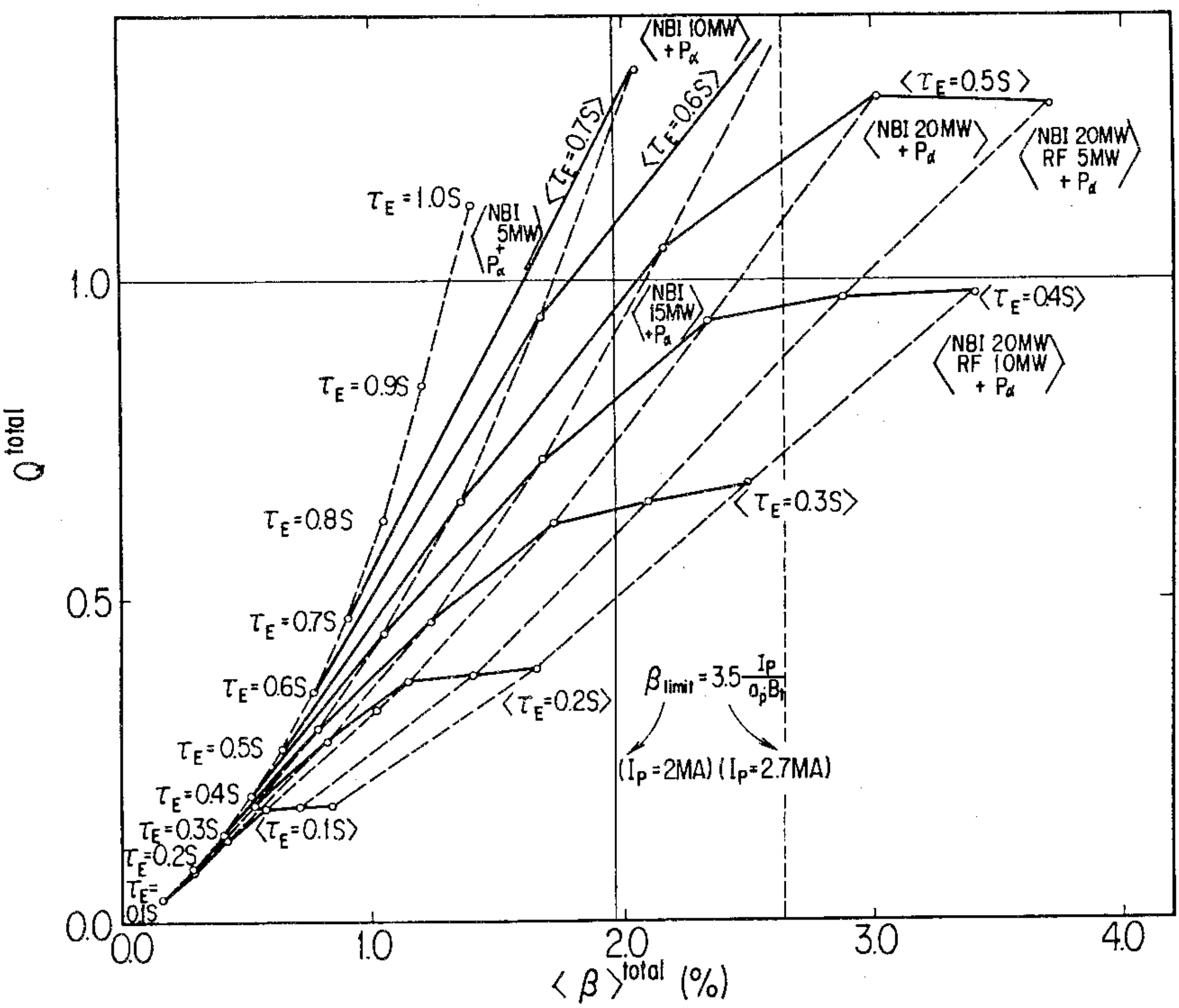

FIG. 6 Q^{total} versus $\langle\beta\rangle^{total}$ at $\bar{n}_e=6\times10^{19}$ m^{-3}, E_B=100 keV, $n_D^{th}:n_T^{th}$ =1:1, R_p=3.15 m, a_p=0.83 m, B_T=4.3T and q_a=2.34. Solid lines indicate τ_E constant case. Dashed lines denote auxiliary heating power constant case. Troyon β-limits for I_p=2 MA and 2.7 MA are also indicated.

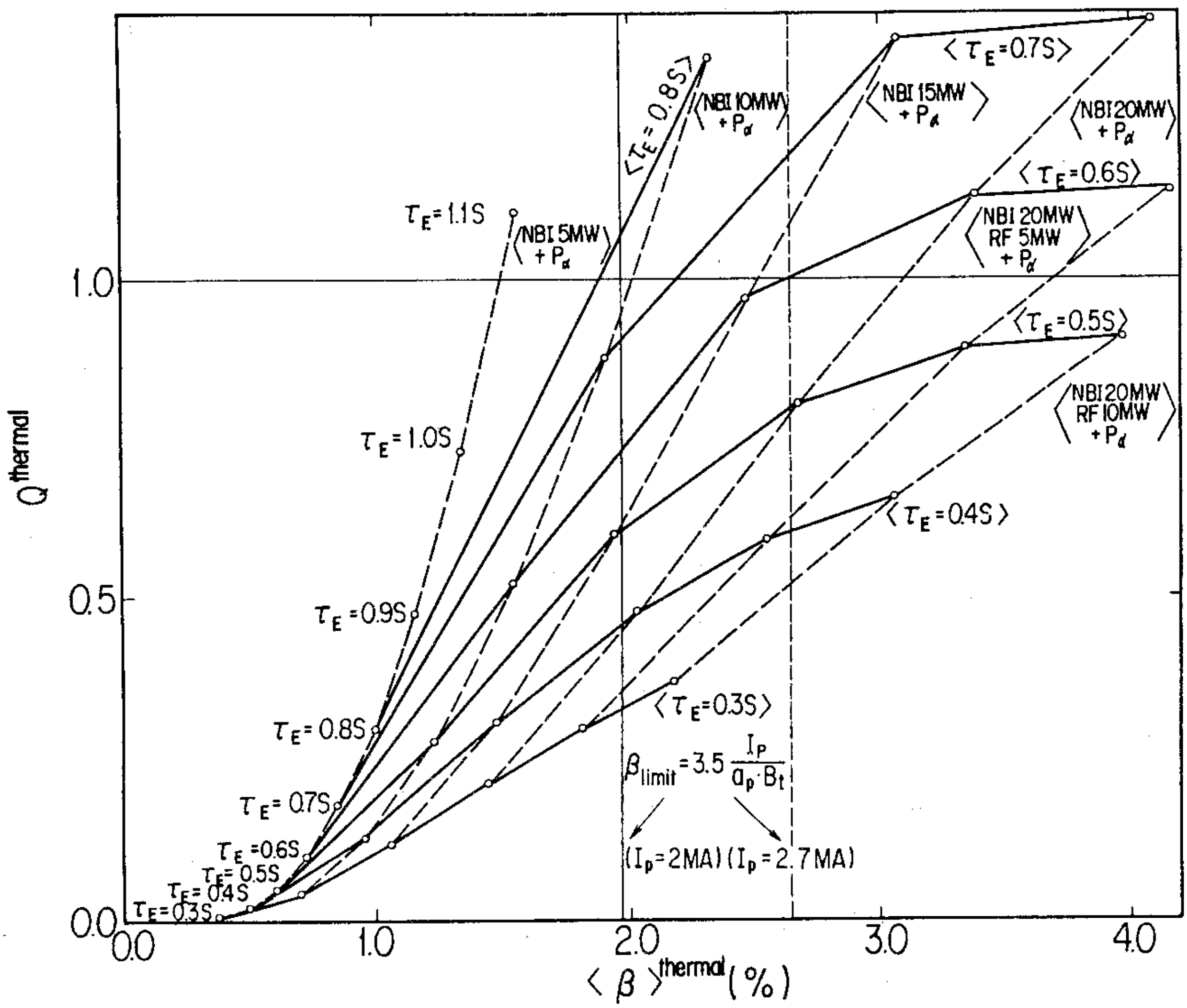

FIG. 7 $Q^{thermal}$ versus $\langle\beta\rangle^{thermal}$ at $\bar{n}_e = 6\times10^{19}$ m^{-3}, E_B=100 keV, $n_D^{th}:n_T^{th}$=1:1, R_p=3.15 m, a_p=0.83 m, B_T=4.3T and q_a=2.34. Solid lines indicate τ_E constant case. Dashed lines denote auxiliary heating power constant case. Troyon β-limits for I_p=2 MA and 2.7 MA are also indicated.

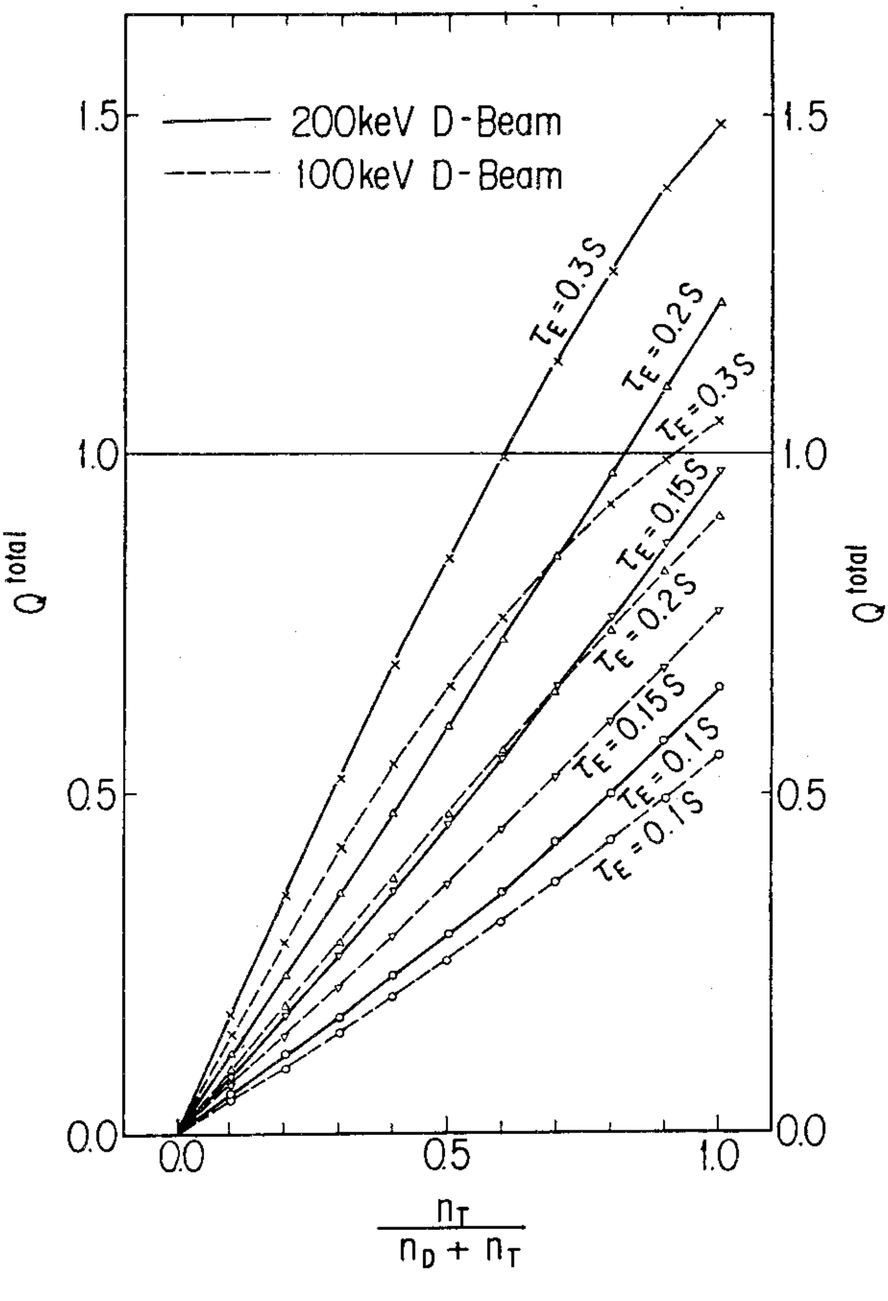

FIG. 8 Q^{total} as a function of $n_T^{th}/(n_D^{th}+n_T^{th})$ which is the ratio of tritium density to deuterium plus tritium densities as a function of various energy confinement times at $\bar{n}_e=4\times10^{19}$ m^{-3}, P_B^{abs}(=20 MW) + $P_{\dot{\alpha}}$, R_p=3.15 m, a_p=0.83 m, B_T=4.3T and I_p=2 MA. Q^{total} by 100 keV deuterium beam is indicated by dashed line and that by 200 keV deuterium beam is represented by solid line.

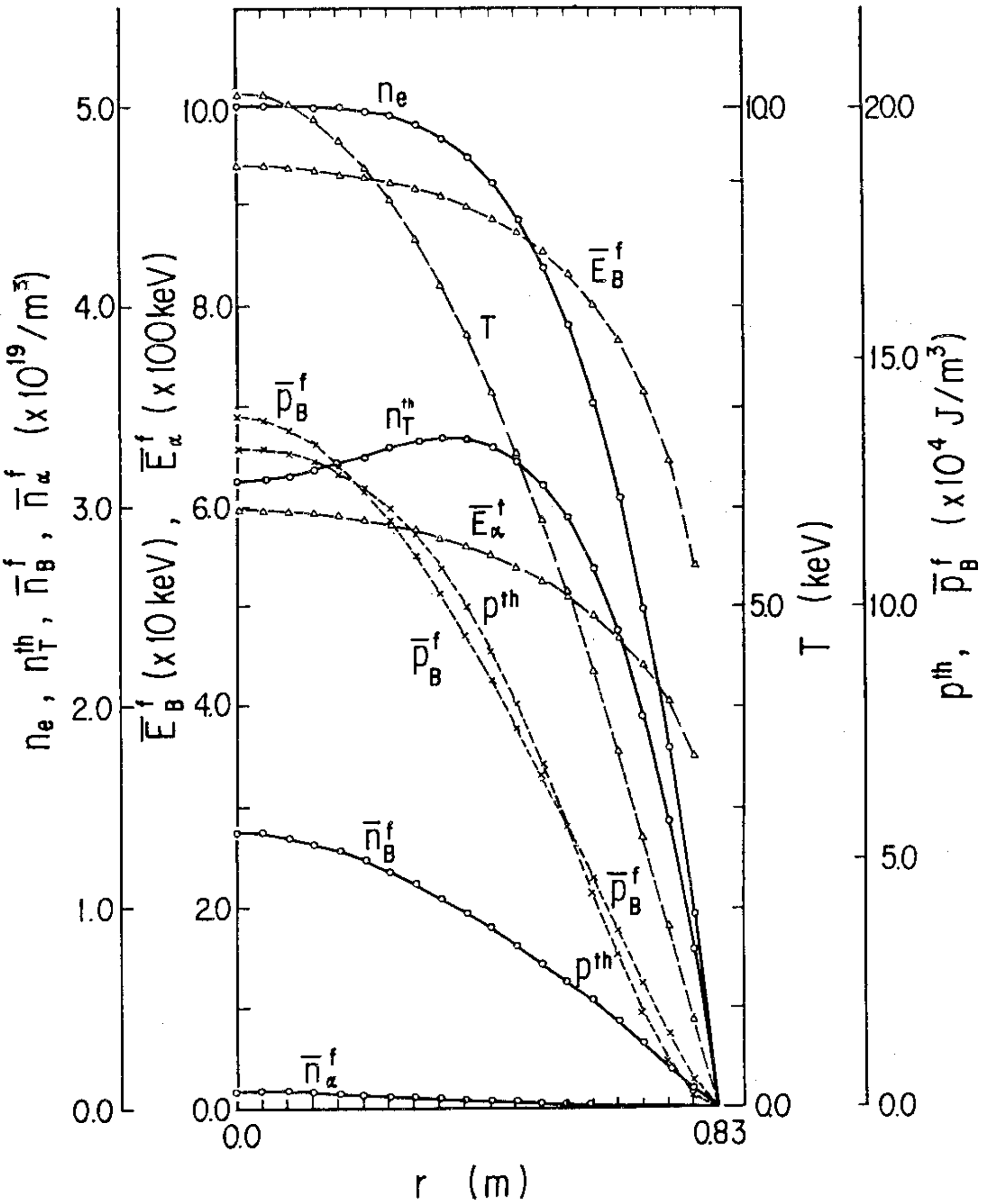

FIG. 9 Radial profiles of plasma density (n_e, n_D^{th}, n_T^{th}), stored fast ion density ($\bar{n}_B^f$, $\bar{n}_\alpha^f$), plasma temperature (T), velocity space averaged beam and α particle energy ($\bar{E}_B^f$, $\bar{E}_\alpha^f$), thermal plasma pressure (p^{th}), and velocity space averaged beam fast ion pressure ($\bar{p}_B^f$) at τ_E=0.15 sec, $\bar{n}_e$=4×10¹⁹ m⁻³, P_B^{abs}(=20MW)+P_α, E_B=200 keV, n_D^{th}:n_T^{th}=0:1, R_p=3.15 m, a_p=0.83 m, B_T=4.3T and I_p=2 MA resulting Q^{total}=0.98 and $\langle\beta\rangle^{total}$=1.54%.

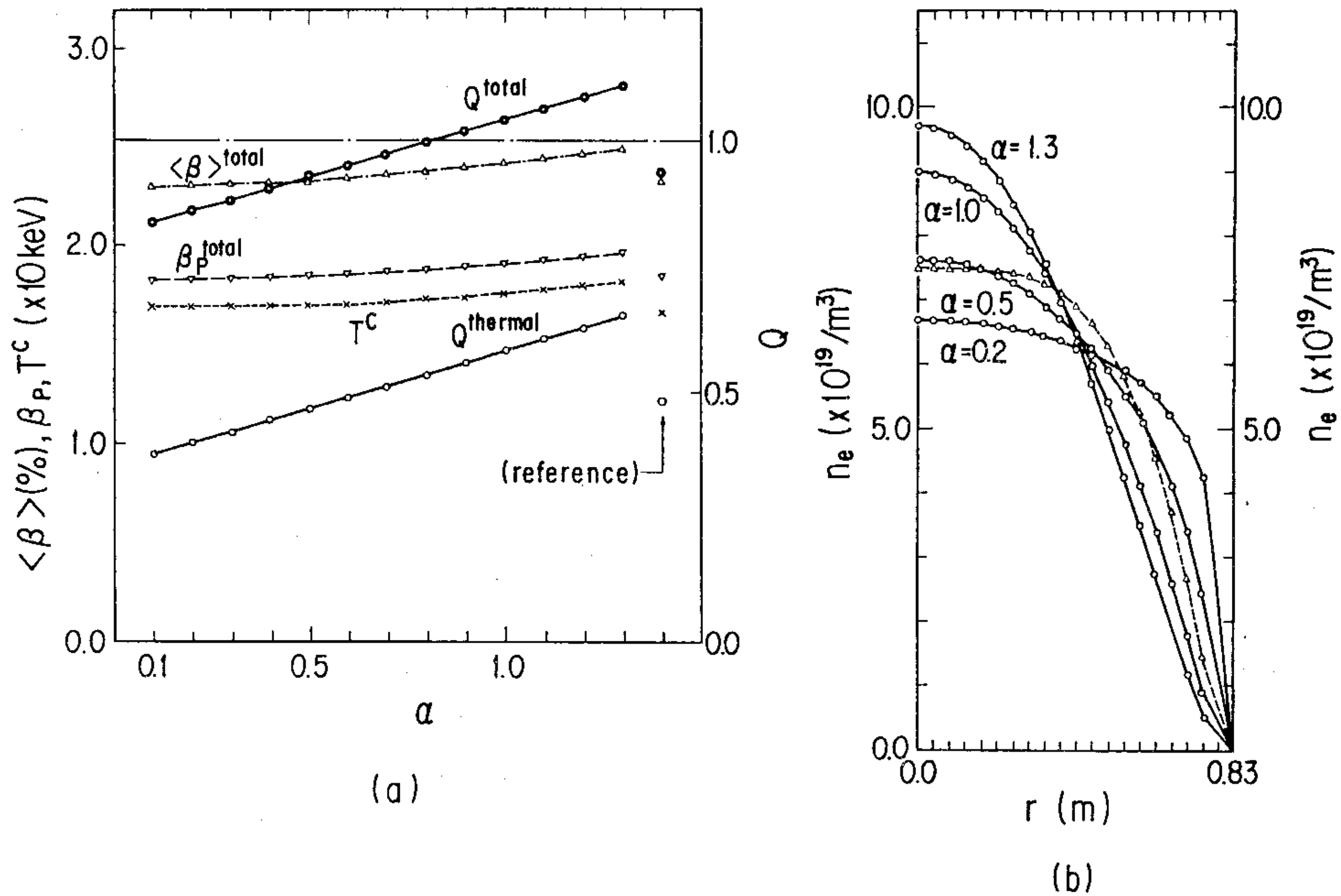

FIG. 10 (a) Dependency of Q^{total}, $Q^{thermal}$, $\langle\beta\rangle^{total}$, β_p^{total} and T^c on density index α at τ_E=0.4 sec, $\bar{n}_e=6\times10^{19}$ m^{-3}, P_B^{abs} (=20MW)+P_α, E_B=100 keV, $n_D^{th}:n_T^{th}$=1:1, R_p=3.15 m, a_p=0.83 m, B_T=4.3 T and I_p=2 MA. (b) Typical radial profiles of electron densities with index α.

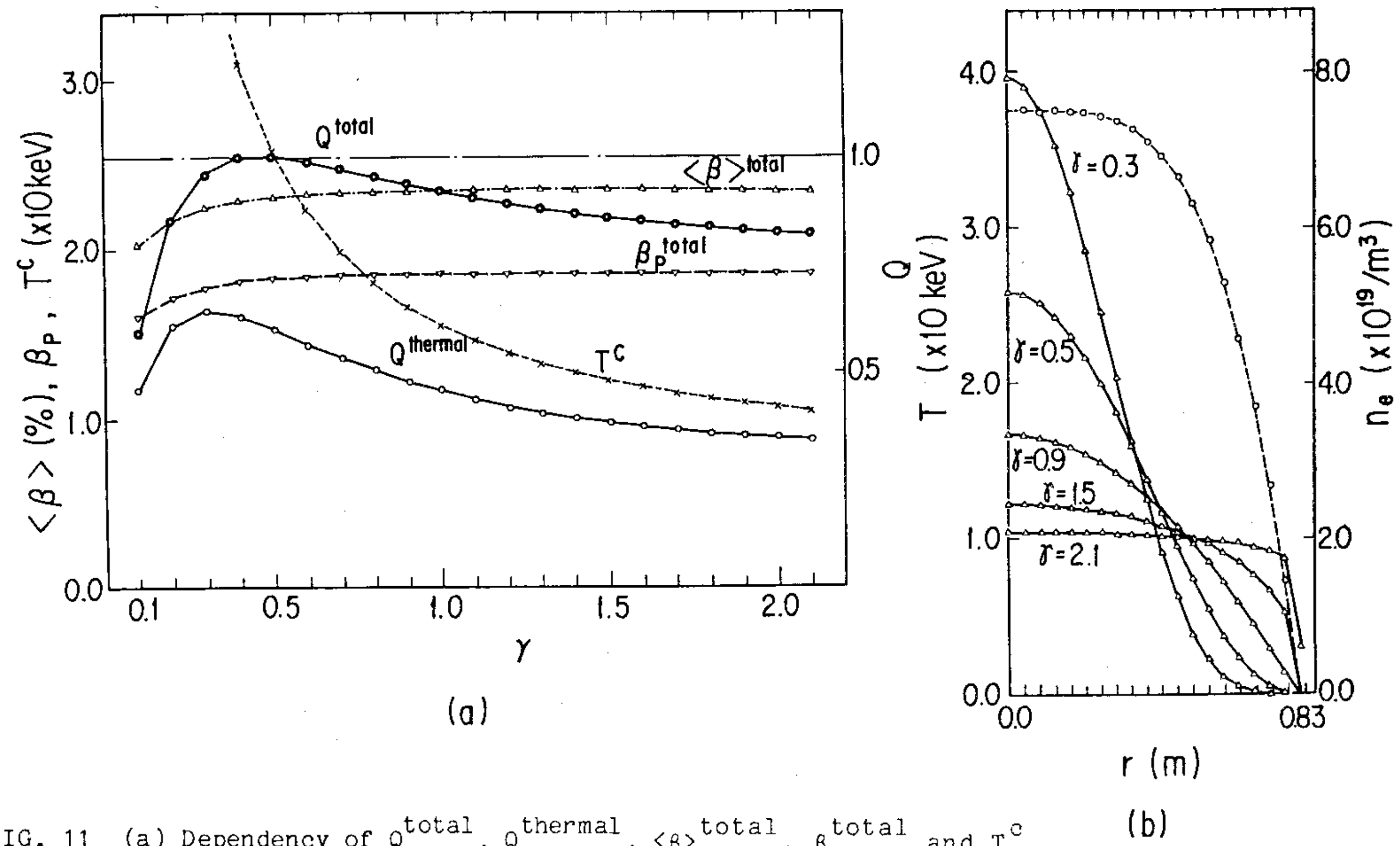

FIG. 11 (a) Dependency of Q^{total}, $Q^{thermal}$, $\langle\beta\rangle^{total}$, β_p^{total} and T^c on plasma temperature radial profile parameter γ at τ_E=0.4 sec, $\bar{n}_e$=6×10^{19} m^{-3}, P_B^{abs}(=20MW)+P_α, E_B=100 keV, $n_D^{th}:n_T^{th}$=1:1, R_p=3.15 m, a_p=0.83 m, B_T=4.3 T and I_p=2 MA. (b) Typical radial profiles of plasma temperature with parameter γ by solid lines. Dashed line shows radial profile of electron density.

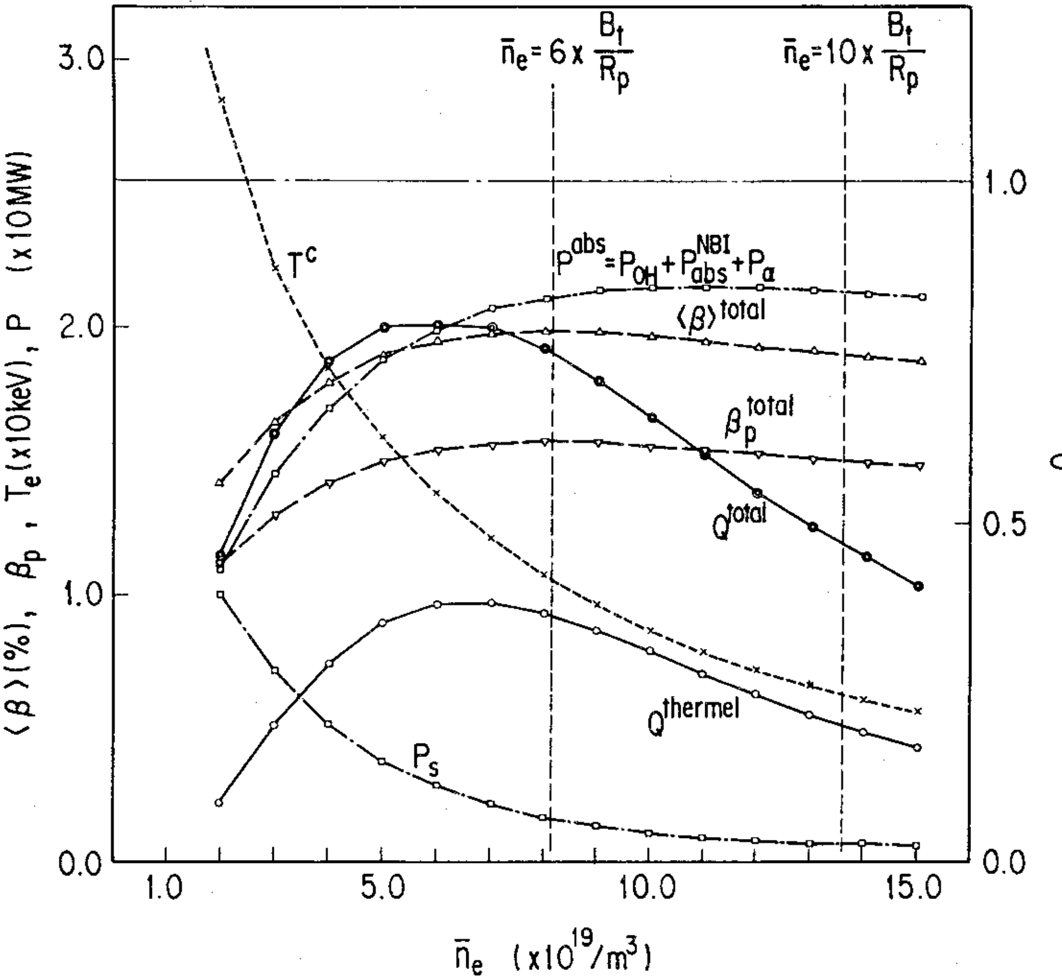

FIG. 12 Effect of beam deposition. Density dependence of Q^{total}, $Q^{thermal}$, $\langle\beta\rangle^{total}$, β_p^{total}, T^c, absorbed power into plasma P^{abs} and shine through loss P_s at τ_E=0.4 sec, P_B^{inj}(=20MW)+P_α, E_B=100 keV, $n_D^{th}:n_T^{th}$=1:1, R_p=3.15 m, a_p=0.83 m, B_T=4.3 T and I_p=2 MA. We neglect charge exchange loss, orbit loss and ripple loss. Line averaged electron densities for Murakami factors which correspond to 6.0 and 10.0 are also indicated.

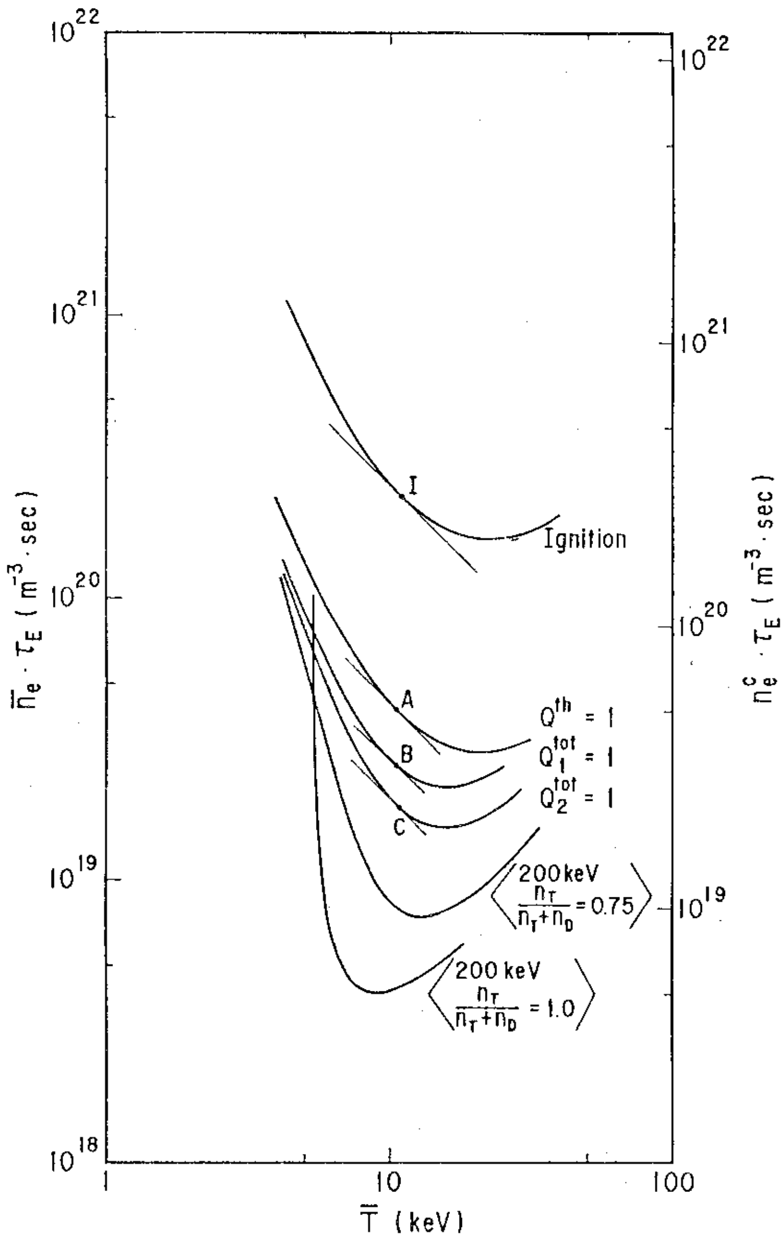

FIG. 13 nτT diagram for ignition condition and break-even conditions. We consider three break-even conditions by only thermal D-T reaction and by thermal D-T reaction including TCT effect with 100 keV and 200 keV deuterium beam at Z_{eff}=1.5 and $n_T^{th}/(n_T^{th}+n_D^{th})$=0.5. Point where each condition's line touches nτT constant line has the minimum nτT value and is indicated as symbol A, B, C and I. Q^{total}=1 considering TCT effect with 200 keV deuterium beam for $n_T^{th}/(n_T^{th}+n_D^{th})$=0.75 or 1.0 is also indicated.

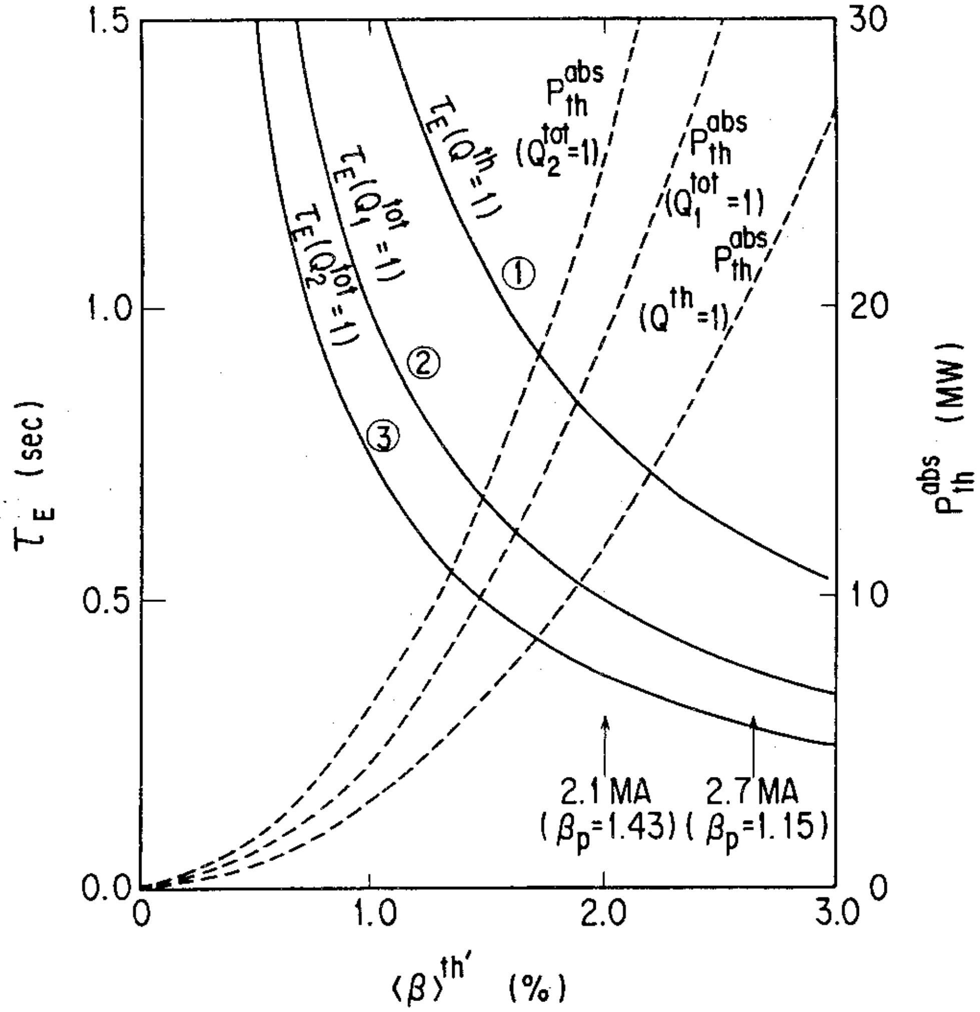

FIG. 14 Relation between energy confinement time and averaged toroidal beta values which means the plasma pressure where all particles are thermalized at B_T=4.3 T for the minimum $n\tau T$ values by only thermal D-T reaction and by thermal D-T reaction including TCT effect with 100 keV and 200 keV deuterium beam. Absorbed power to thermal plasma P_{th}^{abs} for 43 m³ of plasma volume is also indicated.

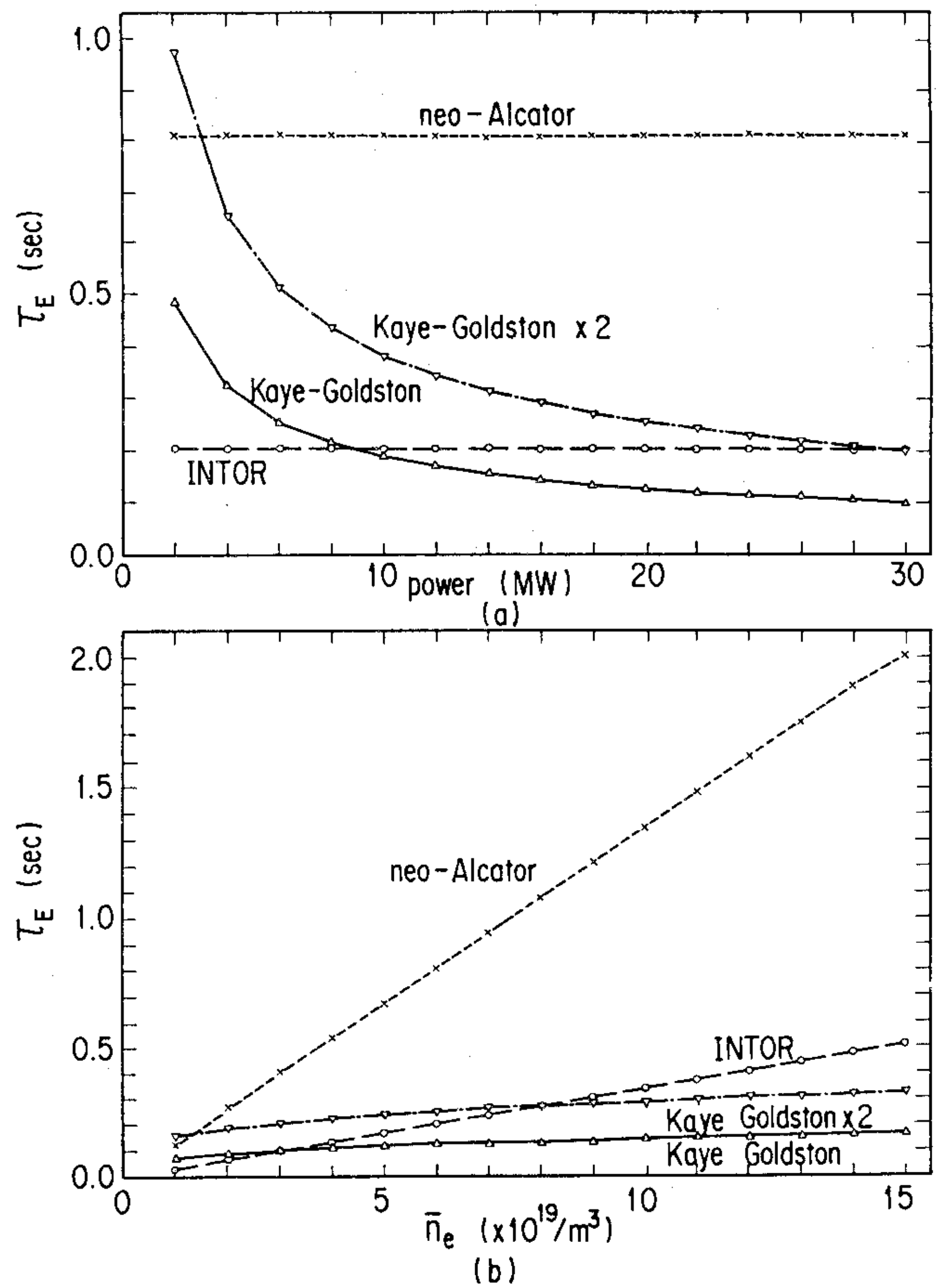

FIG. 15 Various τ_E scaling. (a) Power dependence at $\bar{n}_e=6\times10^{19}$ m^{-3}, $R_p=3.15$ m, $a_p=0.83$ m, $B_T=4.3$ T and $I_p=2$ MA. (b) Density dependence at $P^{abs}=20$ MW, $R_p=3.15$ m, $a_p=0.83$ m, $B_T=4.3$ T and $I_p=2$ MA. Kaye-Goldston $\times$ 2 suggests H-mode scaling.

APPENDIX A FLOW CHART

The main flow chart of this code is described as follows;

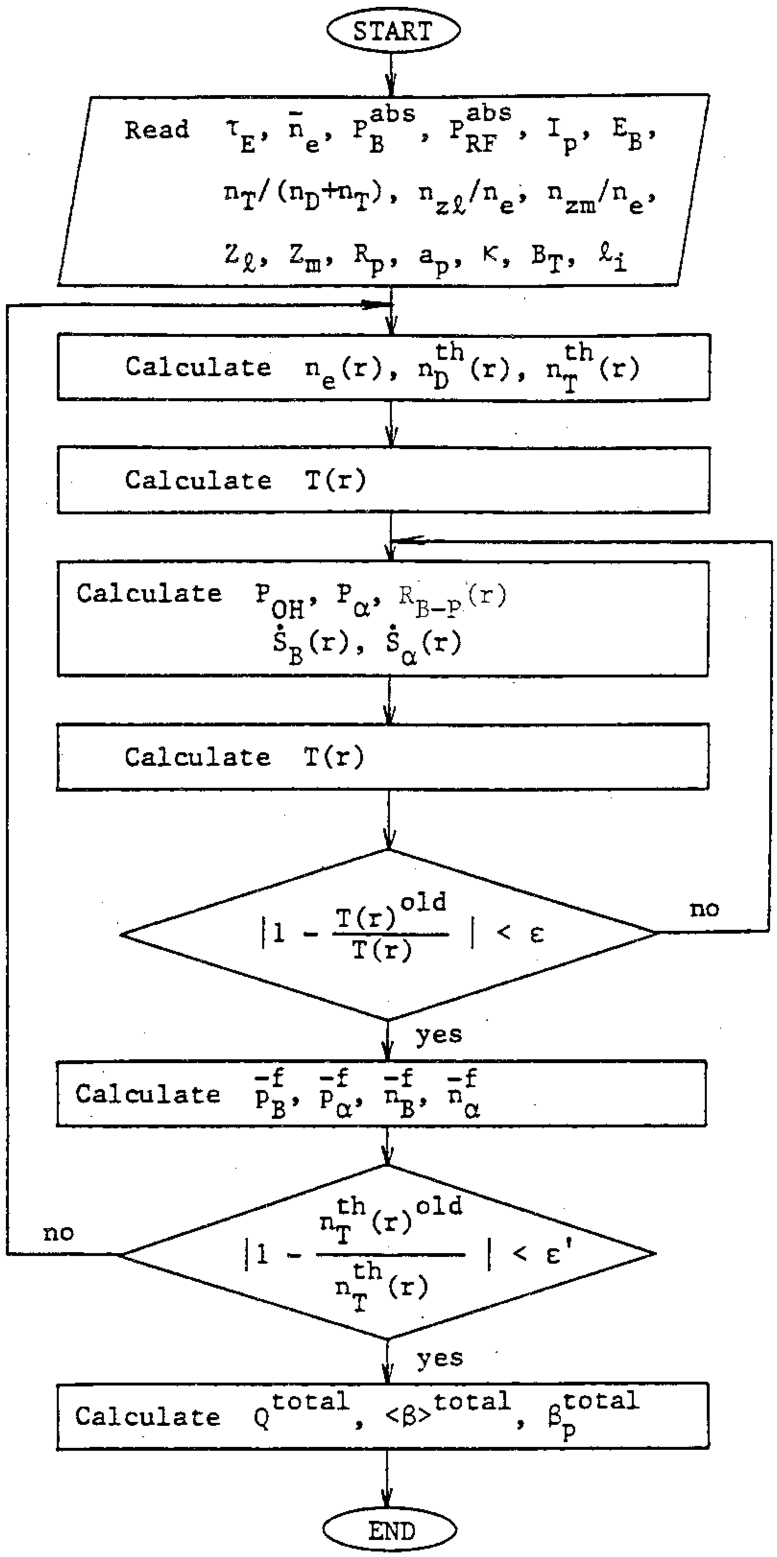

APPENDIX B. BEAM-PLASMA REACTION RATE: R_{B-P}

We assumed that the injected beam particles were trapped fully in the plasma. The energy loss rate by the thermal electrons or ions per one of the beam particles is represented by the following equation under the Fokker-Plank slowing-down model;

$$\left< \frac{dE}{dt} \right>_j^x(E) = \frac{3}{\tau_{se}\sqrt{A_e}} \frac{A_x^{3/2} T_e^{3/2}}{\sqrt{E}\, n_e \, \ell_n \Lambda_e} \frac{n_j z_j^2 \ell_n \Lambda_j}{A_j} X_j F(X_j) \qquad \text{(B-1)}$$

where the suffix x, j mean the injected beam particle and the field particle of all the thermal ions and electron, and the suffix e means electron. τ_{se} is the ion-electron momentum exchange time determined by eq.(8), A is the atomic weight, T_e is the electron temperature, n is the plasma density, E is the injected beam energy during the slowing-down process, and $\ell_n\Lambda$ is the coulomb logarithm. X_j and $F(X_j)$ are determined as follows;

$$X_j = \sqrt{\frac{A_j}{A_x} \frac{E}{T_j}} \qquad \text{(B-2)}$$

$$F(X_j) = \frac{1}{X_j} \int_0^{X_j} e^{-x_j^2}\, dx - \left(1 + \frac{A_j}{A_x} \right) e^{-x_j^2} \qquad \text{(B-3)}$$

When the field particle is electron, $X_j \ll 1$ and $X_j F(X_j) \sim \frac{3}{2} X_j^3$. When the injected beam energy is larger than the thermal plasma energy, $X_j \gg 1$ and $X_j F(X_j) \sim 1$. So, the energy loss rate by all the thermal electrons and ions is simplified approximately from eq.(B-1) as follows;

$$< \frac{dE}{dt} >^{x}(E) = \sum_j < \frac{dE}{dt} >_j^{x} = - \frac{2}{\tau_{se}} \left(\frac{E_c^{3/2} + E^{3/2}}{E^{1/2}} \right) \qquad \text{(B-4)}$$

The fusion reactivity between the Maxwellian thermal tritium plasma and the mono-energy denterium beam ion is described as follows;

$$<\sigma v>_B(E) = \frac{1}{\sqrt{2\pi kT}} \frac{\sqrt{m}_D}{m_T} \frac{1}{\sqrt{E}} \int_0^\infty \sigma(U)\sqrt{U}\{\exp(2\sqrt{\frac{m_T}{m_D}} \frac{\sqrt{E}\sqrt{U}}{T} - \frac{m_T}{m_D}\frac{E}{T} - \frac{U}{T})$$

$$- \exp(-2\sqrt{\frac{m_T}{m_D}} \frac{\sqrt{E}\sqrt{U}}{T} - \frac{m_T}{m_D} \frac{E}{T} - \frac{U}{T})\}dU \quad . \qquad \text{(B-5)}$$

where the suffix T, D mean tritium and deuterium, respectively, and $\sigma(U)$ is the cross-section of D-T reaction.

The reaction energy between the target tritium plasma and the injected beam particle during the slowing down process is

$$E_F = 17.6(\text{MeV})\, n_t \int_{E_{th}}^{E_B} \frac{<\sigma v>_B(E)}{- < \frac{dE}{dt} >^{D}(E)} dE \qquad \text{(B-6)}$$

where E_B is the beam injection energy at the start of the slowing-down process and $E_{th} = \frac{3}{2}$ T is the thermal plasma energy, and n_t is the tritium density of the target plasma. The beam-plasma reaction rate is defined by the following equation;

$$R_{B-P} = \dot{S}_B \, n_t \int_{E_{th}}^{E_B} \frac{\langle \sigma v \rangle_B (E)}{- \langle \frac{dE}{dt} \rangle^D (E)} \, dE \qquad \text{(B-7)}$$

where $\dot{S}_B$ is the beam birth rate. Equation (B-7) corresponds to eq.(19) in the present text. Two equations for $\langle \frac{dE}{dt} \rangle (E)$ as previously mentioned in eq.(B-1) and (B-4) are prepared. We recommend eq.(B-4) since the relative error between eq.(B-1) and eq.(B-4) is less than one percent and the computing time of eq.(B-4) is shorter than that of eq.(B-1). All the integral calculations are carried out using Gaussian's method.

Fig. B-1 shows $Q_B = E_F / E_B$ as a function of deuterium injection energy for various temperatures in the Maxwellian target plasma by 17.6 MeV per reaction. Q_B increases with the plasma temperature since the ion-electron momentum exchange time become long. Q_B depends on n_T / n_e almost linearly and has week dependency on n_e due to $\ell_n \Lambda$.

For reference, the fast ion slowing-down time is described as follows;

$$\tau_s = - \int_{E_{th}}^{E_B} \frac{dE}{\langle \frac{dE}{dt} \rangle^D (E)} = \frac{\tau_{se}}{3} \, \ell_n \left(\frac{E_B^{3/2} + E_c^{3/2}}{E_{th}^{3/2} + E_c^{3/2}} \right) \qquad \text{(B-8)}$$

where E_c is the critical energy during the slowing-down process at which energy being transfered equally to plasma ions and electrons as presented in eq.(11).

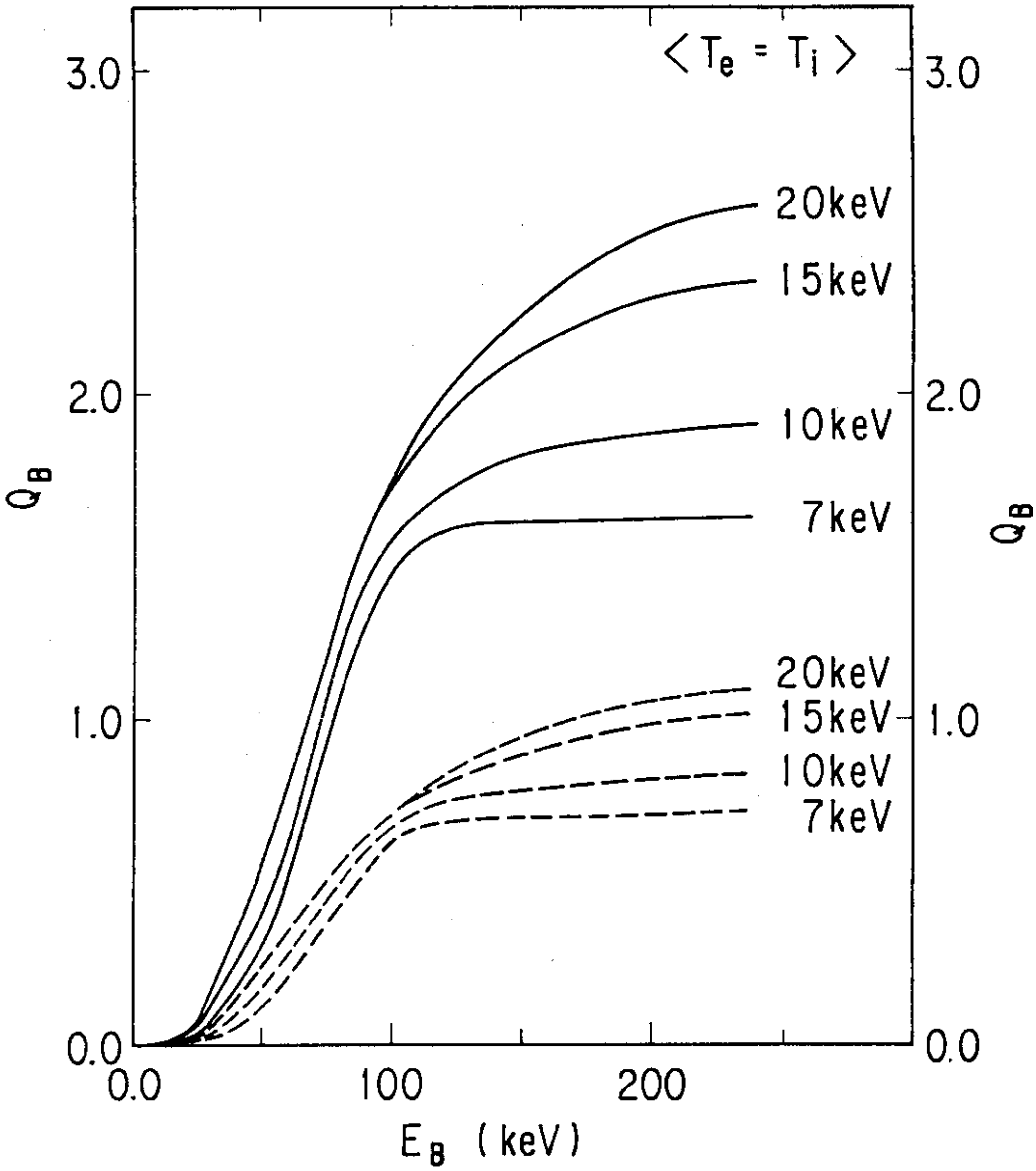

FIG.B-1 Power multiplication factor of the beam-plasma reaction Q_B as a function of deutron injection energy for various plasma temperatures (T_e=T_i) in a Maxwellian target plasma. The case of n_T^{th}=n_e is indicated by solid lines and the case of n_T^{th}=n_D^{th}=$n_e/2$ is demonstrated by dashed lines. 17.6 MeV per reaction.